University of Nebraska - Lincoln
DigitalCommons@University of Nebraska - Lincoln

U.S. Environmental Protection Agency Papers | U.S. Environmental Protection Agency

2014

A novel hybrid approach for estimating total deposition in the United States

Donna B. Schwede
National Exposure Research Laboratory, U.S. Environmental Protection Agency, USEPA, Schwede.donna@epa.gov

Gary G. Lear
U.S. Environmental Protection Agency, Washington, DC

Follow this and additional works at: http://digitalcommons.unl.edu/usepapapers

Schwede, Donna B. and Lear, Gary G., "A novel hybrid approach for estimating total deposition in the United States" (2014). *U.S. Environmental Protection Agency Papers*. 219.
http://digitalcommons.unl.edu/usepapapers/219

This Article is brought to you for free and open access by the U.S. Environmental Protection Agency at DigitalCommons@University of Nebraska - Lincoln. It has been accepted for inclusion in U.S. Environmental Protection Agency Papers by an authorized administrator of DigitalCommons@University of Nebraska - Lincoln.

Atmospheric Environment 92 (2014) 207–220

Contents lists available at ScienceDirect

Atmospheric Environment

journal homepage: www.elsevier.com/locate/atmosenv

A novel hybrid approach for estimating total deposition in the United States

Donna B. Schwede [a,*], Gary G. Lear [b]

[a] Atmospheric Modeling and Analysis Division, National Exposure Research Laboratory, U.S. Environmental Protection Agency, USEPA, MD-E243-02, Research Triangle Park, NC 27711, USA
[b] Clean Air Markets Division, Office of Atmospheric Programs, U.S. Environmental Protection Agency, Washington, DC 20005, USA

HIGHLIGHTS

- A novel approach was developed to produce estimates of total nitrogen and sulfur.
- The approach merges data from measurements and models.
- Measurement data have greater weight near monitoring sites.
- Modeled data are used for deposition species that are not measured.
- This total deposition data set is useful for ecological assessments.

ARTICLE INFO

Article history:
Received 22 October 2013
Received in revised form
4 April 2014
Accepted 7 April 2014
Available online 13 April 2014

Keywords:
Atmospheric deposition
Nitrogen budget
Sulfur budget
Critical loads
Hybrid model

ABSTRACT

Atmospheric deposition of nitrogen and sulfur causes many deleterious effects on ecosystems including acidification and excess eutrophication. Assessments to support development of strategies to mitigate these effects require spatially and temporally continuous values of nitrogen and sulfur deposition. In the U.S., national monitoring networks exist that provide values of wet and dry deposition at discrete locations. While wet deposition can be interpolated between the monitoring locations, dry deposition cannot. Additionally, monitoring networks do not measure the complete suite of chemicals that contribute to total sulfur and nitrogen deposition. Regional air quality models provide spatially continuous values of deposition of monitored species as well as important unmeasured species. However, air quality modeling values are not generally available for an extended continuous time period. Air quality modeling results may also be biased for some chemical species. We developed a novel approach for estimating dry deposition using data from monitoring networks such as the Clean Air Status and Trends Network (CASTNET), the National Atmospheric Deposition Program (NADP) Ammonia Monitoring Network (AMoN), and the Southeastern Aerosol Research and Characterization (SEARCH) network and modeled data from the Community Multiscale Air Quality (CMAQ) model. These dry deposition values estimates are then combined with wet deposition values from the NADP National Trends Network (NTN) to develop values of total deposition of sulfur and nitrogen. Data developed using this method are made available via the CASTNET website.

Published by Elsevier Ltd.

1. Introduction

Atmospheric deposition of sulfur and nitrogen can lead to the decline of ecosystems through acidification (Driscoll et al., 2003; Vitousek et al., 1997) and excess eutrophication (Howarth, 2008; Paerl and Whithall, 1999) which lead to effects such as decreases in forest growth (Aber et al., 2003), loss of species diversity (Bobbink et al., 2010; Driscoll et al., 2001), shifts in the geographical distribution of species (Fenn et al., 2003; Pardo et al., 2011), and increases in harmful algal blooms (Anderson et al., 2008; Heisler et al., 2008; Paerl et al., 2002). In the U.S., strategies for improving ecosystem health often require estimation of the total atmospheric deposition as well as components of the total deposition as input to the analyses. Obtaining estimates of total deposition of sulfur and nitrogen is a challenge in the U.S. due to the difficulty in measuring dry deposition. While modeling of dry

* Corresponding author.
E-mail address: Schwede.donna@epa.gov (D.B. Schwede).

http://dx.doi.org/10.1016/j.atmosenv.2014.04.008
1352-2310/Published by Elsevier Ltd.

This article is a U.S. government work, and is not subject to copyright in the United States.

deposition is done at sites in the Clean Air Status and Trends Network (CASTNET) (Baumgardner et al., 2002), these values cannot be spatially interpolated due to the complexity of the deposition fields. Additionally, several important species that contribute to the nitrogen budget, such as NO_2, N_2O_5, HONO, PANs and alkyl nitrates, are not routinely measured at network sites. Ignoring these species in the calculation of total deposition may result in a significant underestimate of the actual value (Turnipseed et al., 2006). Regional air quality models provide some insight into the concentration and deposition of these compounds, but the characterization of the emissions and atmospheric chemistry of organic nitrogen compounds remains challenging (Cape et al., 2011; Cornell et al., 2003).

Modeling studies of impaired ecosystems, such as critical loads analyses, use biogeochemical models (e.g. Model of Acidification of Groundwater In Catchments (MAGIC) (Cosby et al., 1985), PnET-BGC (Gbondo-Tugbawa et al., 2001)) that require input of an extensive time-series of deposition. While regional air quality models can provide the spatial extent needed, the models have typically been run only for selected years and domains. Additionally, developing consistent emissions inputs for these models for historical periods remains a challenge although recent efforts such as Xing et al. (2013) have made progress in this area. Development of a multi-year data set of total deposition for the US would fill an important need of these ecological analyses.

In response to this need, we developed a novel approach for estimating total deposition in the US. This hybrid approach allows for spatially and temporally continuous estimates of total deposition to be derived for the years 2000–2012, with an extension to later years as monitoring data become available. Data from monitoring networks is used as well as model outputs from the Community Multiscale Air Quality (CMAQ) model (Byun and Schere, 2006). The methodology gives precedence to measurements and supplements with modeled data as needed to provide a complete budget. In the following sections, we provide a description of the total deposition (TDEP) data sets and methodology used to develop estimates of total deposition as well as a discussion of the outputs derived from this technique.

2. Methodology

In this hybrid approach to using monitoring and modeling data to derive estimates of total deposition, data was obtained from monitoring networks in the US for the years 2000–2012. Modeled data was obtained from the CMAQ model for the years 2002–2009.

2.1. Measurement data

Measured values for air concentration and precipitation chemistry were obtained from U.S. national monitoring networks. A map showing the locations of the network sites used in this study is provided in Fig. 1. Table 1 provides a summary of the measurement values used from each of the networks. A full site list with periods of operation is provided in the Supplemental Material. The Clean Air Status and Trends Network (CASTNET), coordinated by the U.S. Environmental Protection Agency, measures atmospheric sulfur and nitrogen species (SO_2, HNO_3, and particulate SO_4^{2-}, NO_3^- and NH_4^+) on a weekly basis using a 3-stage filter pack at over 80 rural sites across the U.S. for evaluation of air quality programs and examining long-term trends in concentration and deposition (U.S. Environmental Protection Agency, 2013c). Biweekly measurements of atmospheric ammonia concentrations are made using Radiello passive samplers by the Ammonia Monitoring Network (AMoN) operated by the National Atmospheric Deposition Program (NADP) (National Atmospheric Deposition Program, 2012). AMoN measurements began in 2007 and the number of sites has grown to over 50 in recent years. Data from AMoN for 2008–2012 are used in this study. The South Eastern Aerosol Research and Characterization (SEARCH) network is operated by Atmospheric Research and Analysis, Inc. (Atmospheric Research and Analysis Inc. (ARA), 2012). The sampled species, frequency and site locations have varied from year to year. The initial version of the total deposition maps includes HNO_3, SO_2, and NH_3 from 2005 to 2011 for the rural sites in the SEARCH network. For the initial version of the TDEP data, networks were selected that conformed to a continuous sampling schedule. Future versions will likely include data from additional networks such as Interagency Monitoring of Protected Visual Environments (IMPROVE) (Colorado State University, 2014).

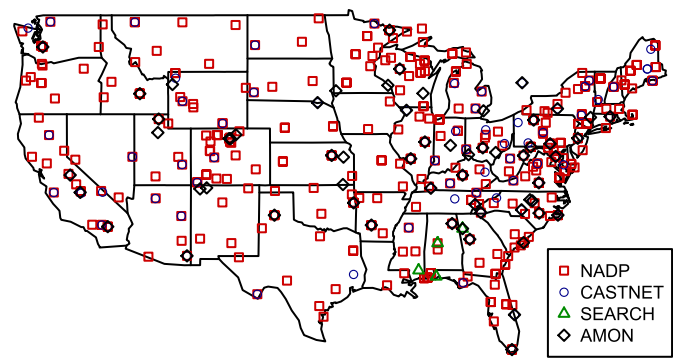

Fig. 1. Map of NADP, CASTNET, SEARCH, and AMoN sites used in the analysis. Not all sites were operational for the entire period 2000–2012.

Precipitation chemistry was obtained from the National Trends Network (NTN) operated by NADP (National Atmospheric Deposition Program, 2012). NTN collects weekly precipitation samples and measures a number of analytes including SO_4^{2-}, NO_3^- and NH_4^+. The measured values of precipitation chemistry are then combined with precipitation estimates from the Parameter-elevation Regression on Independent Slopes Model (PRISM) (PRISM Climate Group (PRISM), 2012) to obtain weekly estimates of wet deposition. Since NADP measurements are relatively sparse, PRISM is used to improve the development of wet deposition grids by accounting for effects of complex climate regimes such as occur in mountainous terrain and coastal areas.

2.2. Modeled data

CMAQ is an advanced regional air quality model that simulates the complex physics and chemistry of the atmosphere to predict

Table 1
Summary of data from monitoring networks used in the methodology.

Network	Chemical species	Period of record	Website
CASTNET	Concentration: HNO_3, SO_2, pSO_4, pNO_3, pNH_4	2000–2012	http://epa.gov/castnet/javaweb/index.html
AMON	Concentration: NH_3	2008–2012	http://nadp.sws.uiuc.edu/AMoN/
SEARCH	Concentration: HNO_3, SO_2, NH_3	2005–2011	http://www.atmospheric-research.com/studies/SEARCH/
NTN	Wet deposition: SO_4, NO_3, NH_4	2000–2012	http://nadp.sws.uiuc.edu/NTN/

Table 2
Summary of CMAQ model runs used in the methodology.

Year	CMAQ Model version (grid resolution)	Emission Inventories						Met model	Land use classification
		NEI[a]	Major point sources	Mobile sources (model)	Fires	Biogenic	Ag		
2002	4.7 (36 km)	2002	2002	2002 (MOBILE 6)	2002	2002	2002	MM5	USGS 24
2003	4.7 (36 km)	2002	2003	2003 (MOBILE 6)	2003	2003	2002	MM5	USGS 24
2004	4.7 (36 km)	2002	2004	2004 (MOBILE 6)	2004	2004	2002	MM5	USGS 24
2005	4.7 (36 km)	2002	2005	2005 (MOBILE 6)	2005	2005	2002	MM5	USGS 24
2006	4.7 (36 km)	2002	2006	2006 (MOBILE 6)	2006	2006	2002	MM5	USGS 24
2007	4.7.1 (12 km)	2005	2007	2007 (MOVES)	2007	2007	2002	WRF	NLCD 2001
2008	4.7.1 (12 km)	2008	2008	2008 (MOVES)	2008	2008	2008	WRF	NLCD 2001
2009	4.7.1 (12 km)	2009	2009	2009 (MOVES)	2009	2009	2008	WRF	NLCD 2001

[a] NEI = National Emissions Inventory (http://www.epa.gov/ttn/chief/eiinformation.html).

the simultaneous transport, transformation, and deposition of pollutants (Byun and Schere, 2006). The model requires gridded fields of meteorological variables which are typically provided by the Weather Research and Forecasting (WRF) model (Skamarock et al., 2008) or its predecessor, MM5 (Grell et al., 1995). Gridded, speciated emissions information is provided via the SMOKE processing system (UNC, 2013). We were able to take advantage of a long series (2002–2009) of CMAQ runs that were done in support of the Centers for Disease Control and Prevention (CDC) Public Health Air Surveillance Evaluation (PHASE) study (Center for

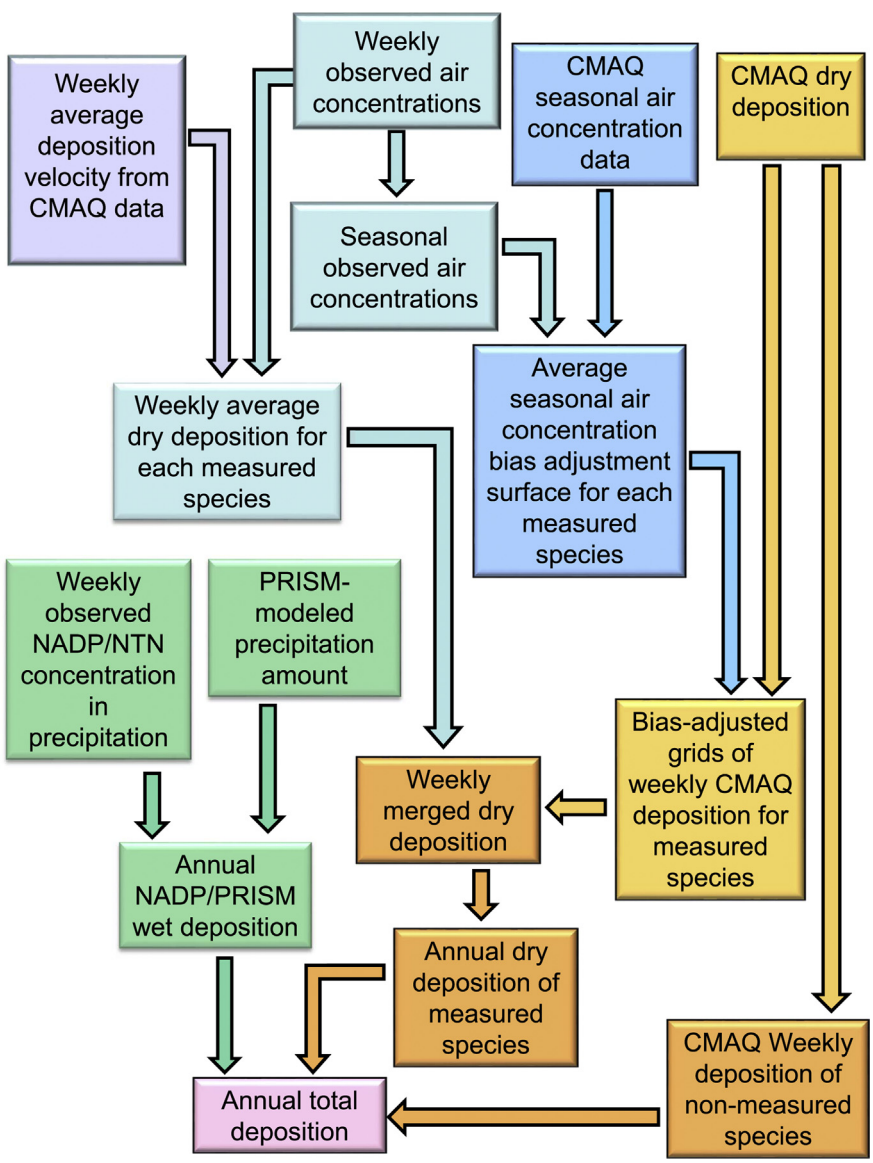

Fig. 2. Flowchart outlining the steps in the methodology from data input to creation of estimates of total annual deposition. Color coding denotes different data streams. (For interpretation of the references to colour in this figure legend, the reader is referred to the web version of this article.)

Table 3
Maximum radius used in the inverse distance weighting to produce concentration grids and the development of distance weighting grids.

Chemical species	Maximum radius (km)			
	Winter	Spring	Summer	Fall
HNO_3	394.6	477.0	229.0	381.5
NH_3	41.9	109.6	84.6	58.4
SO_2	288.5	271.5	232.8	305.4
pNO_3	582.3	583.5	192.5	407.0
pNH_4	538.8	564.3	425.7	563.0
pSO_4	538.8	564.3	425.7	563.0

Disease Control and Prevention, 2013) to develop the needed gridded fields for this methodology. While we used CMAQ in this effort, other air quality models could be used with this methodology. CMAQ concentration, deposition velocity and deposition values are predicted for a large number of pollutants. For this study, we used deposition flux, deposition velocity and concentration values for HNO_3, SO_2, NH_3, and particulate species and deposition values for HNO_3, NO, NO_2, N_2O_5, HONO, PANs, and organic nitrate (NTR in CMAQ).

For the years 2002–2006, CMAQ v4.7 was run using a 36-km × 36-km grid cell size for the conterminous United States (CONUS) domain. All 36-km CMAQ grids were re-gridded to 12-km grids. Year specific meteorology was obtained from the MM5 model. Emissions were developed using the 2002 National Emissions Inventory (NEI), with year specific emissions for major point sources, mobile sources, and fires. The specifics details of these runs are presented in Appel et al. (2011). CMAQ v4.7.1 was run for 2007–2009 using a 12-km grid spacing for the CONUS domain. Meteorology for each year was obtained from the WRF model. For 2007, the 2005 NEI was used for emissions with year specific emissions for major point sources, mobile sources, and fires, while agricultural emissions from the 2002 NEI emissions were used (Hall et al., 2012a). Emissions for 2008 and 2009 were developed from the 2008 NEI, including agricultural sources, with year specific

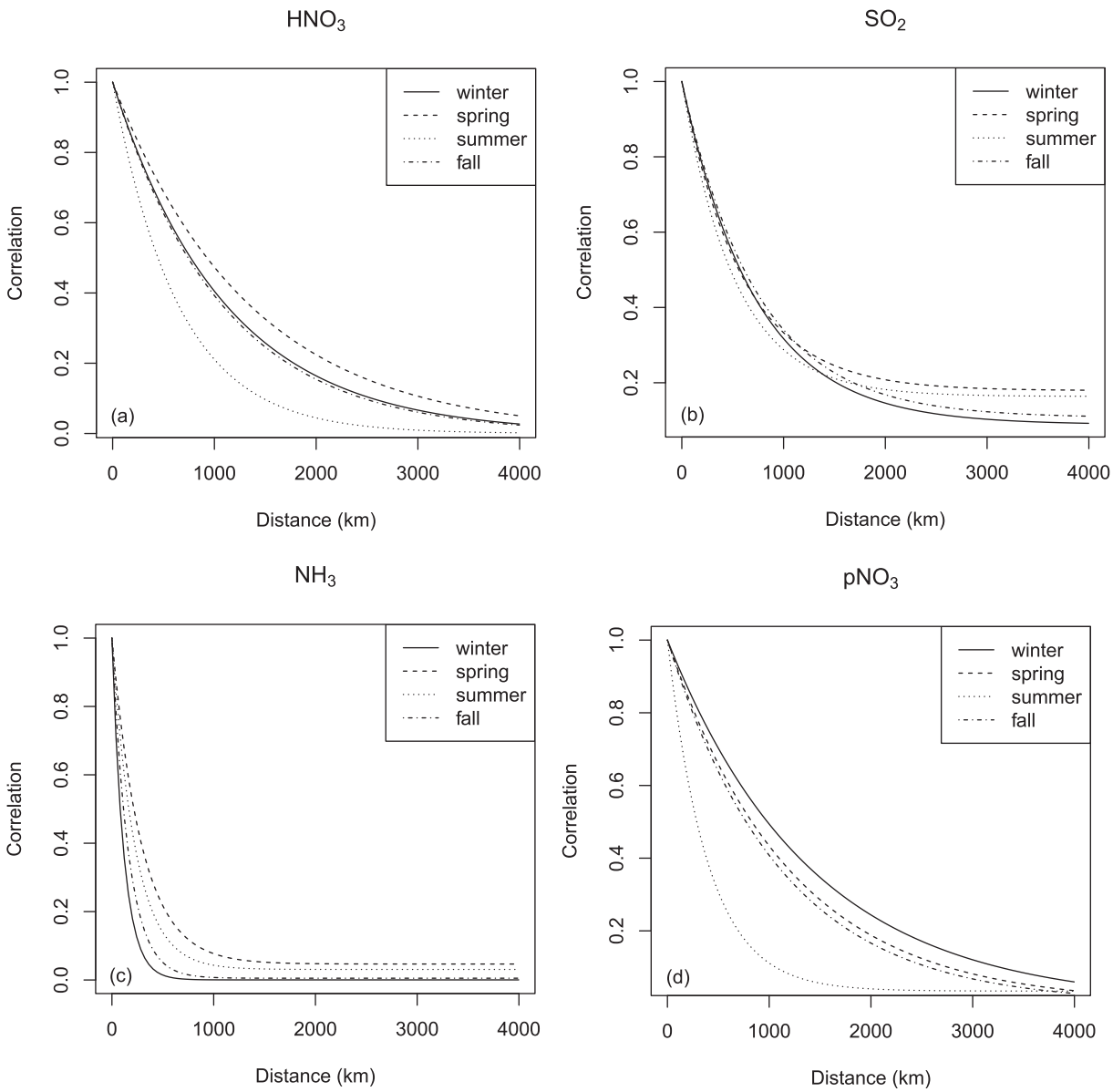

Fig. 3. Normalized covariance based on seasonal average concentrations from CMAQ for 2008 for (a) HNO_3, (b) SO_2, (c) NH_3, and (d) pNO_3.

emissions for major point sources, mobile sources, and fires (Hall et al., 2012b; U.S. Environmental Protection Agency, 2013a). A different temporal allocation was used for the agricultural emissions for the 2009 data compared to the 2008 data. A summary of these model runs is provided in Table 2 and complete details can be found in the references provided. The current release of CMAQ (v5.0.1) contains additional model options that were not available in earlier versions. These include a bidirectional flux model for NH_3 and the ability to include NO from lightning. Updates have also been made to the emissions processing system and the current

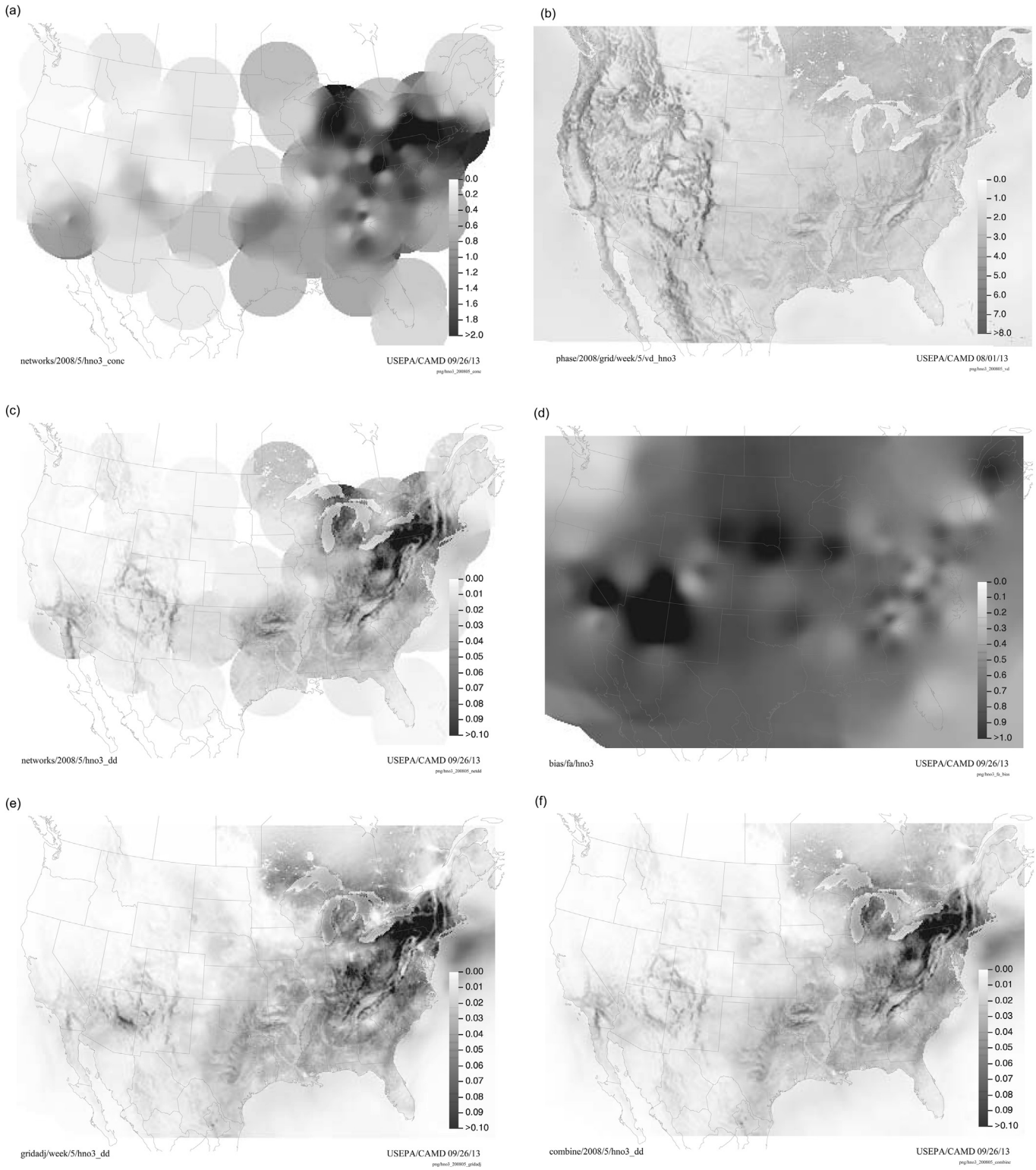

Fig. 4. Example intermediate output from the data processing for HNO_3 for week 5 of 2008: (a) merged and gridded concentration field from measured values ($\mu g\ m^{-3}$), (b) CMAQ deposition velocity ($cm\ s^{-1}$), (c) deposition calculated from multiplying observed concentrations by CMAQ deposition velocity (kg-N ha^{-1}), (d) bias ratio (observed/CMAQ), (e) CMAQ bias adjusted dry deposition (kg-N ha^{-1}), and (f) deposition from merging modeled and observed (kg-N ha^{-1}).

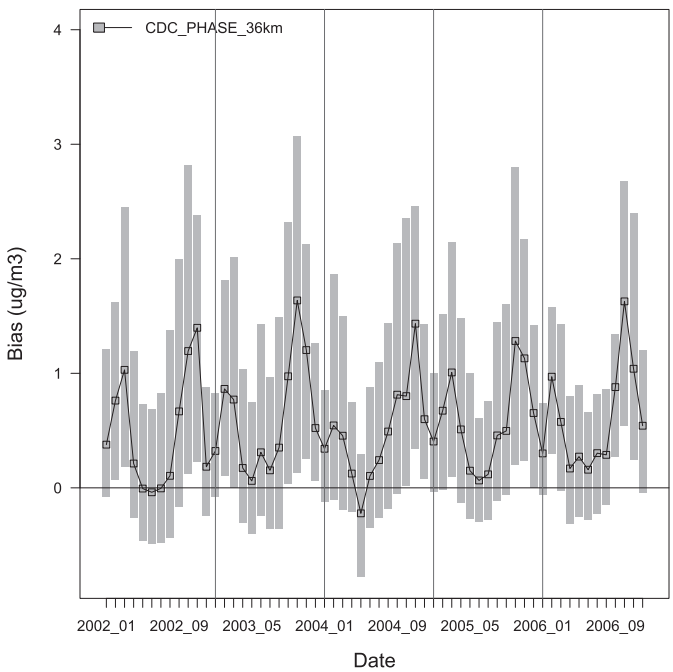

Fig. 5. Bias (μg m^{-3}) in CMAQ total nitrate concentration from the CDC PHASE model runs for the CONUS domain compared to CASTNET sites for the years 2002–2006. Grey bars denote the 25th and 75th percentiles. Circles and black lines indicate median value for the month of all weekly concentrations at all sites.

version contains a revised temporal profile for confined animal feed lot emissions. Future work will include investigating the effects of using these model options on the total deposition estimates as well as the effects of using higher resolution model output for all years.

Table 4
List of output variables.

Variable	Description	Units
NH_3	Dry deposition of ammonia	kg-N/ha
pNH_4	Dry deposition of particulate ammonium	kg-N/ha
SO_2	Dry deposition of sulfur dioxide	kg-S/ha
pSO_4	Dry deposition of	kg-S/ha
Dry N	Total dry deposition of nitrogen	kg-N/ha
Dry N (pct of total)	Total dry deposition of nitrogen as percent of total (wet + dry) deposition	Percent
Total N	Total (wet + dry) nitrogen deposition	kg-N/ha
Other N	Dry deposition of unmeasured nitrogen species	kg-N/ha
Other N (pct of total)	Dry deposition of unmeasured nitrogen species as percent of total (wet + dry) deposition	Percent
Dry oxN	Dry deposition of oxidized nitrogen	kg-N/ha
Dry oxN (pct of total)	Dry deposition of oxidized nitrogen as percent of total (wet + dry) deposition	Percent
Total oxN	Total (wet + dry) deposition of oxidized nitrogen	kg-N/ha
Total oxN (pct of total)	Total (wet + dry) deposition of oxidized nitrogen as percent of total (wet + dry) deposition	Percent
Dry reN	Dry deposition of reduced nitrogen	kg-N/ha
Dry reN (pct of total)	Dry deposition of reduced nitrogen as percent of total (wet + dry) deposition	Percent
Total reN	Total (wet + dry) deposition of reduced nitrogen	kg-N/ha
Total reN (pct of total)	Total (wet + dry) deposition of reduced nitrogen as percent of total (wet + dry) deposition	Percent
Dry S	Total dry deposition of sulfur	kg-S/ha
Dry S (pct of total)	Total dry deposition of sulfur as percent of total (wet + dry) deposition	Percent
Total S	Total (wet + dry) sulfur deposition	kg-S/ha

2.3. Combining the data

The data from the monitoring networks and model output were combined in a multistep process that is outlined in Fig. 2 and detailed below. The first step in the methodology is the development of gridded weekly concentration fields of sulfur dioxide (SO_2), nitric acid (HNO_3), ammonia (NH_3), particulate sulfate (pSO_4), particulate nitrate (pNO_3), and particulate ammonium (pNH_4) using the monitoring data. Measured air concentrations from CASTNET, SEARCH and AMoN are not natively on the same sampling schedule; therefore, all measured air concentrations were converted to the standard CASTNET Tuesday–Tuesday week. The measured data were then interpolated into grids using inverse-distance weighting (IDW). The maximum distance of influence used in the IDW were determined from examining the spatial correlation in the CMAQ gridded average seasonal concentration data using a variogram analysis. For each chemical and season, we plotted the sample variogram and then fitted an exponential covariance model with three parameters (nugget, sill, and range) using a nonlinear least squares algorithm. The covariance model was then normalized and plotted against distance. Distances corresponding to a covariance of 0.7 were determined for each chemical species for each season (Table 3) and used in the IDW. Plots of normalized covariance for several species are shown in Fig. 3. An example grid resulting from interpolating the concentration data is shown in Fig. 4a for HNO_3 for week 5 of 2008.

Next, CMAQ hourly deposition velocity grids were aggregated to the CASTNET weekly schedule to obtain average weekly values. Deposition velocity cannot be interpolated across varying land use types, so explicit calculations for each grid cell are needed as is provided by CMAQ. Year-specific grids were developed as well as average grids for 2002–2004 and 2007–2009. Fig. 4b shows the average deposition velocity surface for week 5 of 2008 for HNO_3.

The third step in the methodology is the creation of gridded fields of weekly dry deposition for each measured species using the gridded measured concentrations and modeled deposition velocities. For the years 2002–2006, the year-specific weekly average concentration grids were multiplied by the year-specific weekly average deposition velocity grids for each species. For the years 2000–2001, modeled deposition velocities were not available. Therefore, the year-specific weekly average concentration was multiplied by the weekly average deposition velocities determined from the years 2002–2004. This reduces the effect of one outlier year overly influencing the deposition velocity estimate. Similarly, for the years 2010–2012, the year-specific weekly average concentration was multiplied by weekly average deposition velocities determined from the years 2007–2009. An example grid of HNO_3 dry deposition is shown in Fig. 4c. The calculations for particulate species require special treatment. The CASTNET sampling system uses an open-faced filter pack without a specific size cut for particulate species. CMAQ uses a modal aerosol model with three modes (Aitken (I), accumulation (J), and coarse (K)). For pSO4, deposition was calculated using the deposition velocity for the CMAQ accumulation mode. Since pNO_3 is known to be bimodal, but the specific percentages in each mode in the measured data were not known, the deposition velocity was calculated as a weighted average assuming 80% is in the accumulation mode and 20% is in the coarse mode. For pNH_4, we assumed it is associated 80% with pSO_4 and 20% with pNO3, based on molar ratios in CASTNET data, and weighted the deposition velocities accordingly.

The next step in the method is the development of grids of weekly modeled deposition for the measured species. Model evaluation studies such as Appel et al. (2011) and Foley et al. (2010) have indicated that concentration estimates from CMAQ are biased for some species. This bias must be taken into account in the

development of deposition estimates since concentration biases will be carried forward to the dry deposition values. Bias grids were only constructed for species measured by CASTNET because AMoN and SEARCH did not have a sufficient number of observations for the modeled years to estimate the bias of NH_3. We examined the average bias in CMAQ concentration compared to CASTNET and found that the seasonal difference in the bias was more important than the interannual differences or trends (Fig. 5). Therefore, average seasonal bias adjustment grids were calculated by pairing the weekly average monitored value with the weekly average CMAQ concentration in the grid cell that contains it. The bias ratios for each week were then averaged seasonally across the 5-year period. Since the bias surfaces tended to be different for the model runs using the 36-km grid cell (2002–2006) compared to the model runs using the 12-km grid cell (2007–2009), the calculation of seasonal averages was done separately for 2002–2006 and 2007–2009. The bias ratio was transformed to a log scale with ratios capped at 10 to eliminate mathematical effects of very small concentrations and fitted to a surface using IDW with a maximum distance of 1000 km. This distance was selected to ensure that every grid cell in the domain had at least one nearest measurement point included in the IDW. The surface was smoothed using a circular neighborhood mean with a radius of 60 km and then transformed back to the normal scale from the log scale. An example bias surface for HNO_3 in the winter is shown in Fig. 4d.

Next, we created bias-adjusted grids of weekly CMAQ deposition for the CASTNET measured species. CMAQ deposition values for measured species were bias corrected by multiplying the CMAQ value by the ratio obtained in the previous step for the appropriate season. For the years 2000–2006, the average seasonal bias for 2002–2006 was used while the average seasonal bias for 2007–2009 was used for the years 2007–2012. Fig. 4e shows the bias adjusted CMAQ deposition values for HNO_3 for week 5 of 2008.

The next step was to merge the weekly deposition grids from the monitoring data and the CMAQ data for measured species. The process for merging the data preserves the monitoring values at the measurement sites and recognizes that, in areas where there are large spatial extents with no monitoring data, the interpolated measured concentrations may not represent well the variations in emissions and chemical processes that might occur between monitors. For grid cells farther from monitoring locations, the bias-corrected CMAQ values are better able to account for these processes and are given more weight.

To combine these gridded fields, weighting grids were constructed for the observed and modeled deposition grids. First, a grid was constructed that contained the distance from the grid cell to

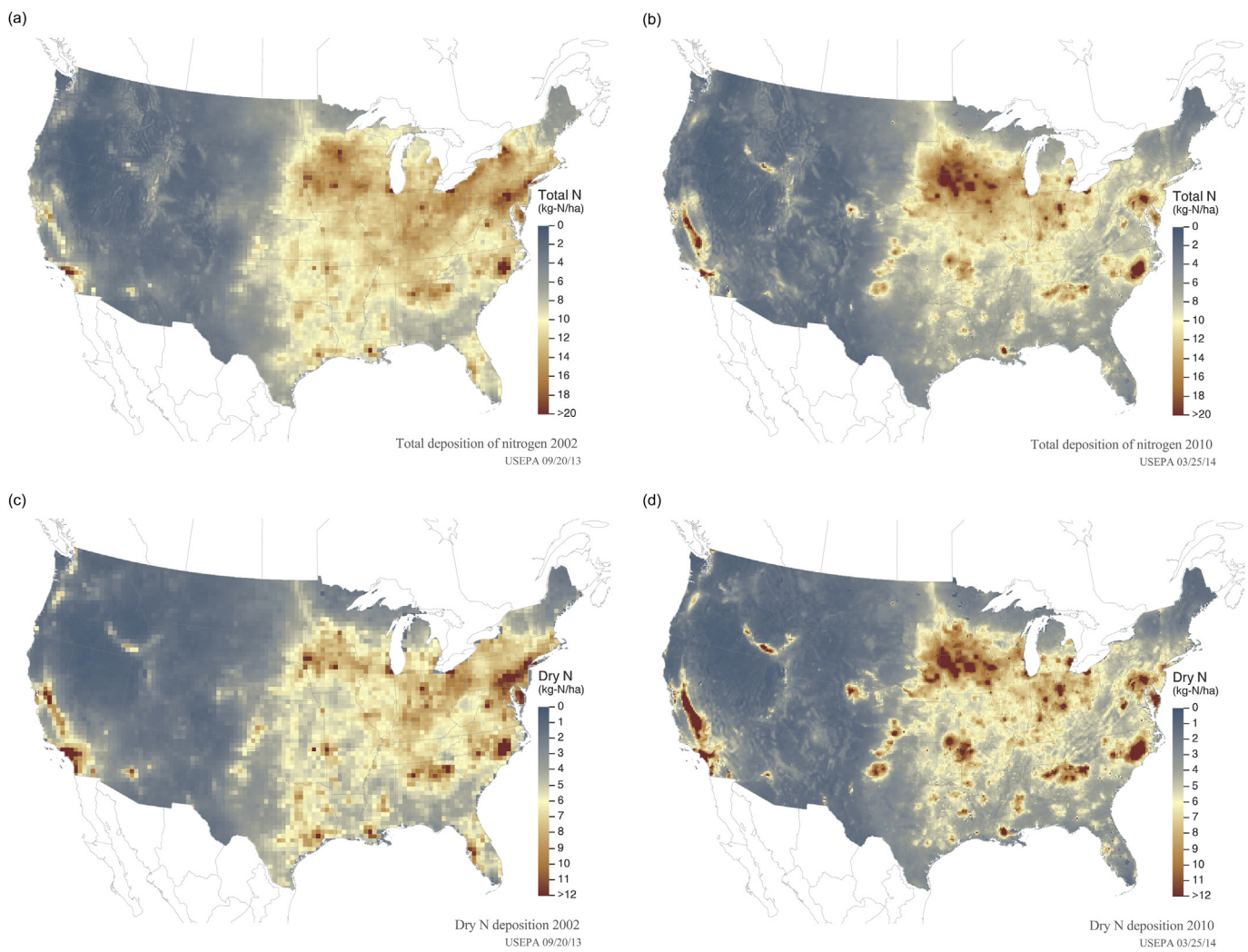

Fig. 6. Total nitrogen deposition (kg-N/ha) calculated using the hybrid approach for (a) 2002 and (b) 2010. Dry nitrogen deposition for (c) 2002 and (d) 2010. Source: CASTNET/CMAQ/NTN/AMON/SEARCH.

the nearest monitor. Next, a distance weighting grid was calculated as

$$W_{\text{obs}} = 1 - \frac{\text{distance to nearest monitor}}{\text{maximum radius}}$$

where the maximum radius was determined for each chemical species based on the variogram analysis described above. The same distances used for inverse-distance weighting the observed concentrations were used here as well. The observed deposition grid from above was multiplied by this distance weighting grid to get weighted observed deposition values. The weighting grid for the modeled values was constructed as $1 - W_{\text{obs}}$. The modeled deposition grid for the measured species was multiplied by its weighting grid to get weighted modeled values. The two weighted grids were then summed to get the final deposition grid for each measured species.

To create values for total annual dry deposition, weekly average deposition grids for each species were summed to annual values. For the measured species, the combined weighted deposition grids were summed, while the weekly CMAQ deposition values were summed for unmeasured species (NO, NO_2, N_2O_5, NH_3, HONO, PANs, organic nitrate). For the years 2002–2009, the year-specific annual deposition was used. Years without corresponding CMAQ values were assigned the average annual deposition for the closest year; 2002 for the years 2000–2001 and 2009 for the years 2010–2012. An example grid of annual dry deposition is shown in Fig. 4f.

The final step of the methodology is to combine the annual dry deposition with the annual wet deposition to create grids of total atmospheric deposition. NTN wet deposition values are provided at a 4-km grid resolution. To maintain the spatial variability provided in this data, the 12-km grids of dry deposition were regridded to the 4-km NTN grid. For each year and species, the dry deposition calculated above was summed with the NTN wet deposition to determine total deposition. Additionally, grids of 3-year average deposition for 2000–2002 and 2010–2012 were also calculated.

Admittedly, this method does not maintain mass balance whereas Eulerian models such as CMAQ do. Other efforts that have combined measured wet deposition with bias corrected modeled deposition such as that of Dennis and Foley (2009) suggest that the mass balance error is small. Future work will investigate methods for determining the additional uncertainty in the deposition estimates that is introduced due to the lack of mass balance.

Gridded deposition fields and map images for the variables listed in Table 4 are provided at ftp://ftp.epa.gov/castnet/tdep as compressed ESRI ArcGRID export files. Since this product is

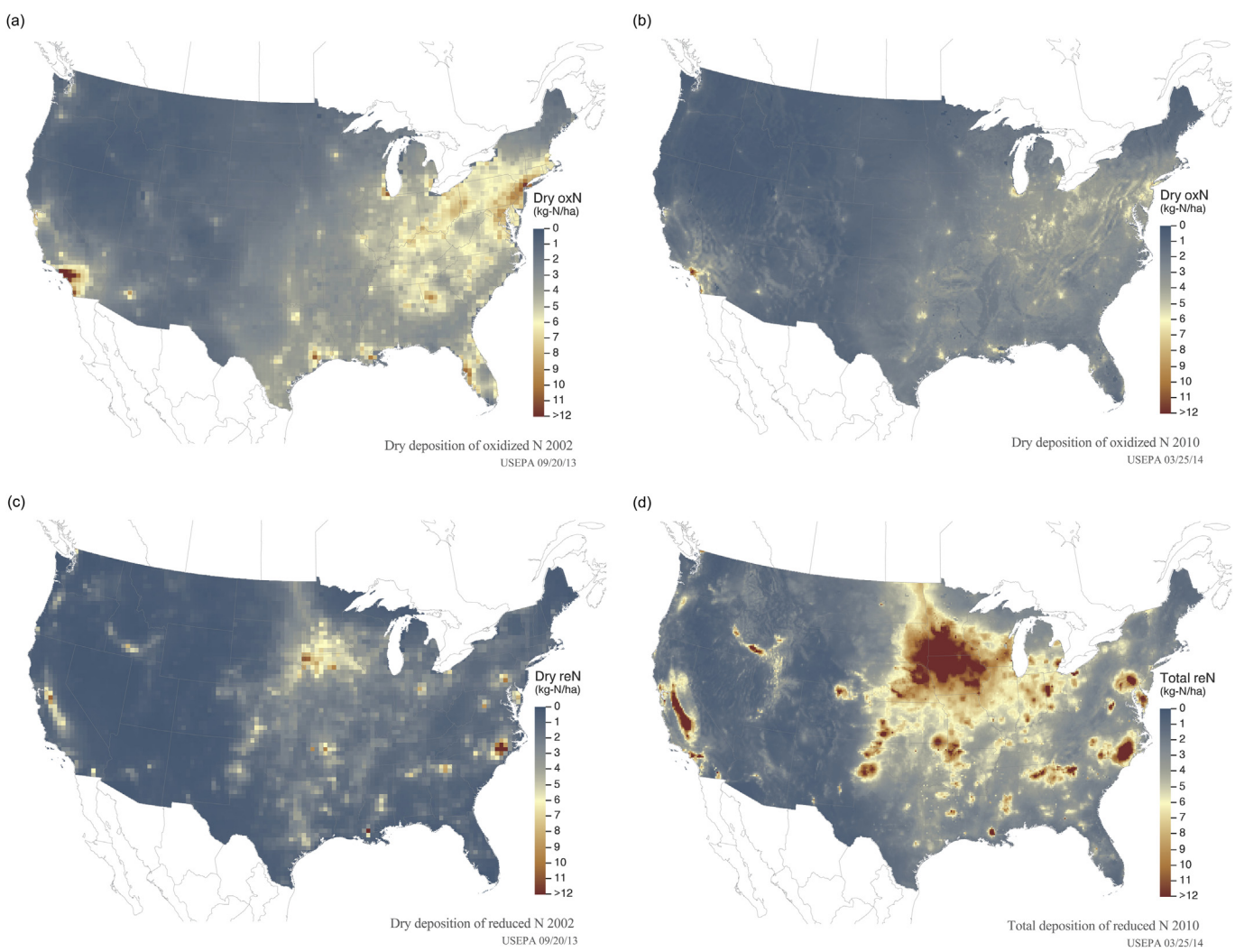

Fig. 7. Oxidized nitrogen dry deposition (kg-N/ha) for (a) 2002 and (b) 2010 and Reduced nitrogen dry deposition (kg-N/ha) for (c) 2002 and (d) 2010 calculated using the hybrid approach.
Source: CASTNET/CMAQ/NTN/AMON/SEARCH.

dynamic with expected updates to the methodology and available measured and modeled data, a version number is associated with the data which includes the four digit year of release and a two digit version number. Using this notation, the release of the data described here is version 2014.01 and contains files for the years 2000–2012. While it would be tempting to use these maps for explicit trends analyses, the lack of consistent emissions and chemical transport modeling platforms makes this problematic. However, with the inclusion of monitored data, the maps likely reflect the overall changes in nitrogen and sulfur deposition that occurred in the time period 2000–2012.

3. Results and discussion

In the following section, we examine some of the maps produced in this effort, discuss features of the maps, and identify areas for future improvements. Additionally, we compare the results of this hybrid approach with other approaches for estimating total deposition. Space limitations preclude the presentation here of all of the maps produced as a result of this project, however a complete set of maps can be downloaded from the FTP site provided above.

3.1. Nitrogen

For nitrogen species, maps and data are available for individual chemical species as well as aggregations such as oxidized and reduced nitrogen. Example maps of dry and total nitrogen deposition for 2002 and 2010 are shown in Fig. 6. In many regions of the US, dry deposition contributes greater than 50% of the total N deposition for both years, however, the contribution of dry deposition to total deposition varies spatially and temporally. As expected, arid areas in the southwest show the highest contribution from dry deposition. The temporal changes between 2002 and 2010 reflect the relative contributions of oxidized and reduced nitrogen. Many of the reductions in total deposition between 2002 and 2010 arise from changes in the oxidized nitrogen as shown in Fig. 7, which is consistent with reductions in NO_x emissions during this period due to air regulations such as the Clean Air Act (U.S. Environmental Protection Agency, 2013b) and the NO_x State Implementation Plan (SIP) call (U.S. Environmental Protection Agency, 2014). The emissions of NH_3 have shown an upward trend from 2002 to 2010 (http://www.epa.gov/ttn/chief/eiinformation.html) and this is reflected in the increased deposition of reduced nitrogen seen in Figs. 6 and 7. These increases are

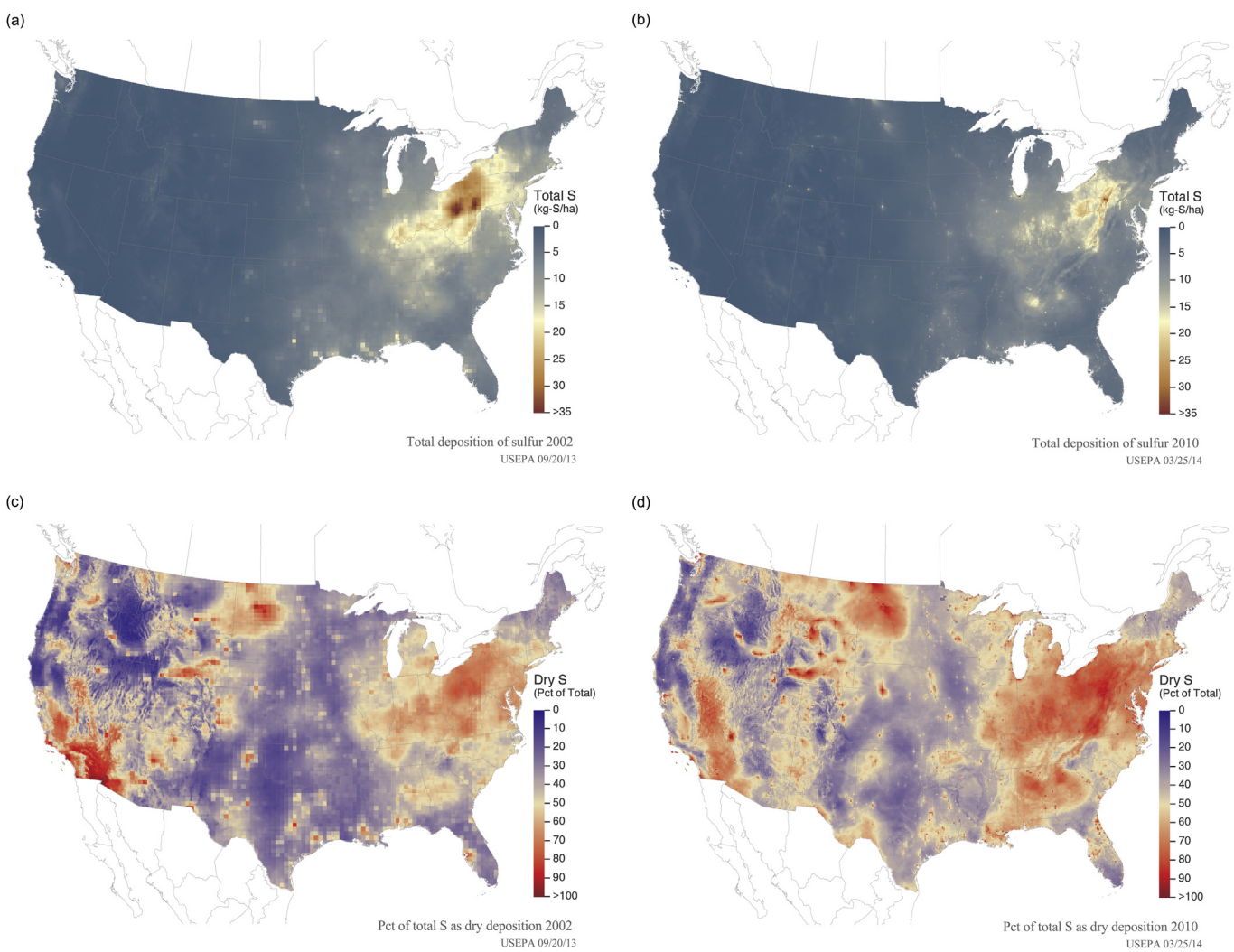

Fig. 8. Total sulfur deposition (kg-S/ha) for (a) 2002 and (b) 2010 and percent contribution of dry sulfur deposition to total sulfur deposition for (c) 2002 and (d) 2010 calculated using the hybrid approach.
Source: CASTNET/CMAQ/NTN/AMON/SEARCH.

due primarily to changes in emissions due to agriculture and include livestock emissions and effects of the increased use of fertilizers on crops. It is important to note that the maps for 2010 include data from the AMoN network while the maps for 2002 do not as the AMoN NH_3 measurements began in 2007. Introduction of the AMoN sites is important for bias correcting CMAQ model output, but can also introduce an artifact making the relative change in reduced nitrogen deposition between 2002 and 2010 appear greater than it may actually be. Without the corresponding AMoN values for 2002, it is difficult to quantify absolutely the change in deposition for specific locations.

The estimates of total deposition include the contribution of the dry deposition of species such as NO, NO_2, N_2O_5, HONO and organic nitrogen as determined by CMAQ. No attempt was made in the current methodology to fuse CMAQ wet deposition estimates of these chemicals with the NADP measurements, although this will be an area for future development. The emission and chemistry of organic nitrogen compounds are not well understood and, therefore, are not currently well represented in air quality models. Some of the organic nitrogen compounds are quite soluble and organic nitrogen is estimated to contribute as much as 30% of the total nitrogen wet deposition (Neff et al., 2002). Less is known about the dry deposition of these compounds. A number of recent studies (e.g. Perring et al., 2013) have shed light on the composition, chemical properties, and deposition properties of organic nitrogen compounds and future versions of CMAQ containing these advancements will be used to update the current methodology and maps. Due to the limited treatment of organic nitrogen in CMAQ v 4.7.1, the values produced in version 2014.01 from this hybrid methodology likely underestimate the organic nitrogen deposition and consequently the total nitrogen deposition.

3.2. Sulfur

For sulfur, maps and data are available for dry, wet, and total deposition of SO_2 and particulate sulfate. We compare sulfur total and dry deposition for 2002 and 2010 in Fig. 8. In Fig. 8a and b, reductions in sulfur deposition from 2002 to 2010, consistent with expectations due to emissions controls, can be seen. SO_2 emissions, primarily from combustion of fossil fuels, decreased by 37% from 2002 to 2010 with the greatest reductions occurring in the northeastern US and the Ohio River Valley area (http://www.epa.gov/air/airtrends/sulfur.html). Similar reductions in deposition can be seen in these areas in Fig. 8. Comparing across years, we see the impact of including the data from the SEARCH network where elevated areas of deposition appear near the SEARCH monitors in Yorkville, GA and Centerville, AL despite trends of decreasing emissions. Data from these sites were not available for the 2002 data set, so

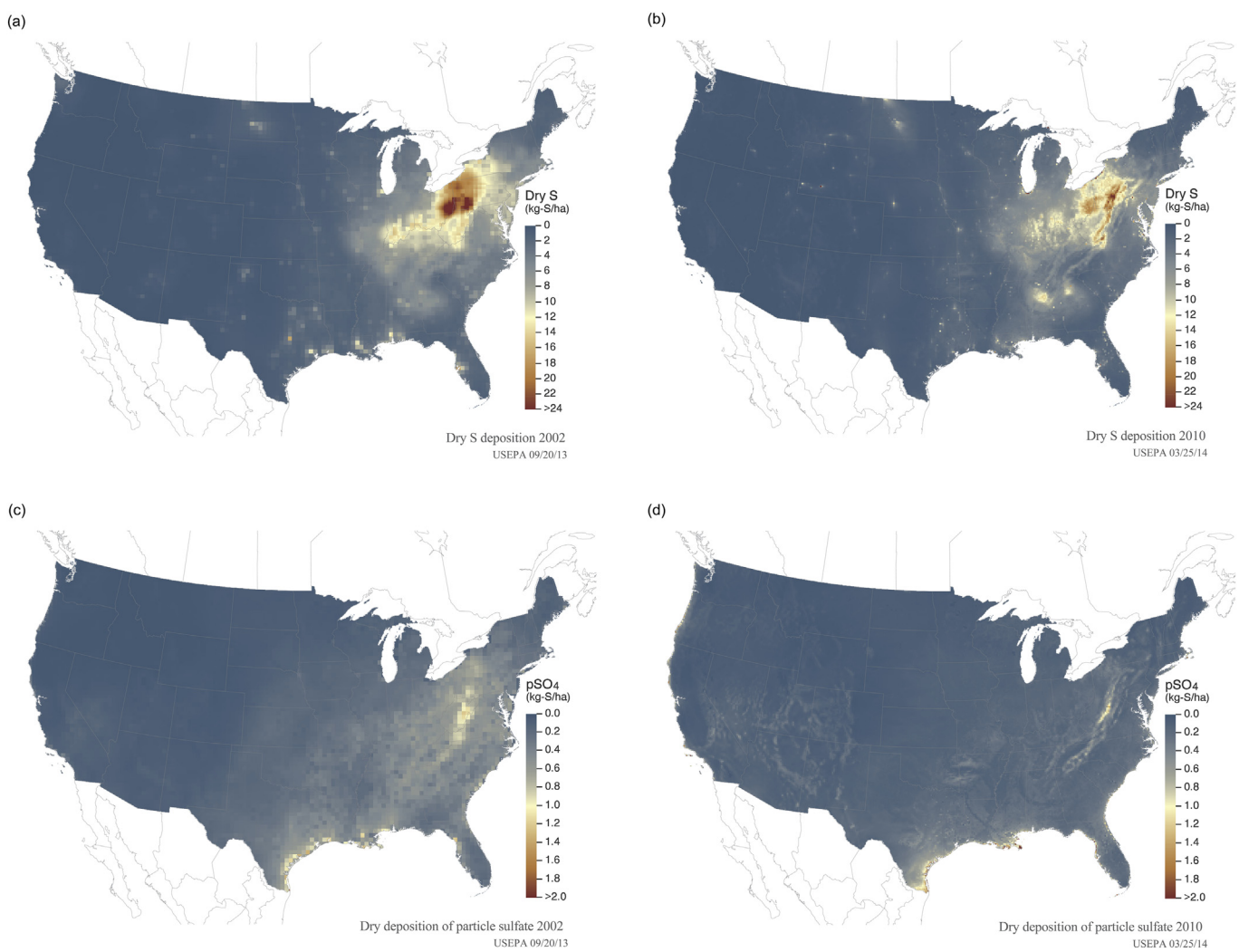

Fig. 9. Dry deposition (kg-S/ha) of SO_2 for 2002 (a) and 2010 (b) and pSO_4 for 2002 (c) and 2010 (d) calculated using the hybrid approach.
Source: CASTNET/CMAQ/NTN/AMON/SEARCH.

including the data, while useful for reducing model bias, creates an artifact. Certainly, having a more spatially and temporally extensive set of monitors would reduce this effect. Fig. 8c and d show the percent contribution of dry deposition to the total deposition. Across the US, the fraction of total deposition contributed by dry deposition is quite spatially and temporally variable. In addition to changes in dry deposition, these spatial and temporal variations reflect differences in precipitation regimes and interannual variability in precipitation amount which influence the contribution of wet deposition. So, although the amount of dry deposition decreases in 2010 compared to 2002, the percent contribution of the dry deposition is higher in 2010 because there was less precipitation and therefore less wet deposition. The dry deposition of individual sulfur species is shown in Fig. 9. Dry deposition of SO_2 is much higher than the dry deposition of pSO_4. Both species show the expected decreases in deposition from 2002 to 2010 that would be expected as a result of air quality regulations that have lowered SO_2 emissions and, therefore, air concentrations.

3.3. Comparison of deposition estimates

Obtaining spatially and temporally continuous estimates of total deposition is challenging since dry deposition is typically measured only for intensive field studies while wet deposition is routinely monitored. One approach that is often used is to combine dry deposition from CASTNET with wet deposition from NTN. For CASTNET, deposition estimates are produced by multiplying site specific concentrations and modeled deposition velocities (Meyers et al., 1998). These estimates cannot be spatially interpolated, however, due to the influence of the underlying land use on the deposition velocity. Spatially continuous estimates of deposition can be obtained from air quality models such as CMAQ, but these estimates can include biases resulting from errors or gaps in emissions and limitations in modeling the complete physics and chemistry of the atmosphere (Appel et al., 2011). In the absence of measured data or estimates from regional air quality models, other approaches for estimating total deposition have been used including assuming that dry deposition equals wet deposition

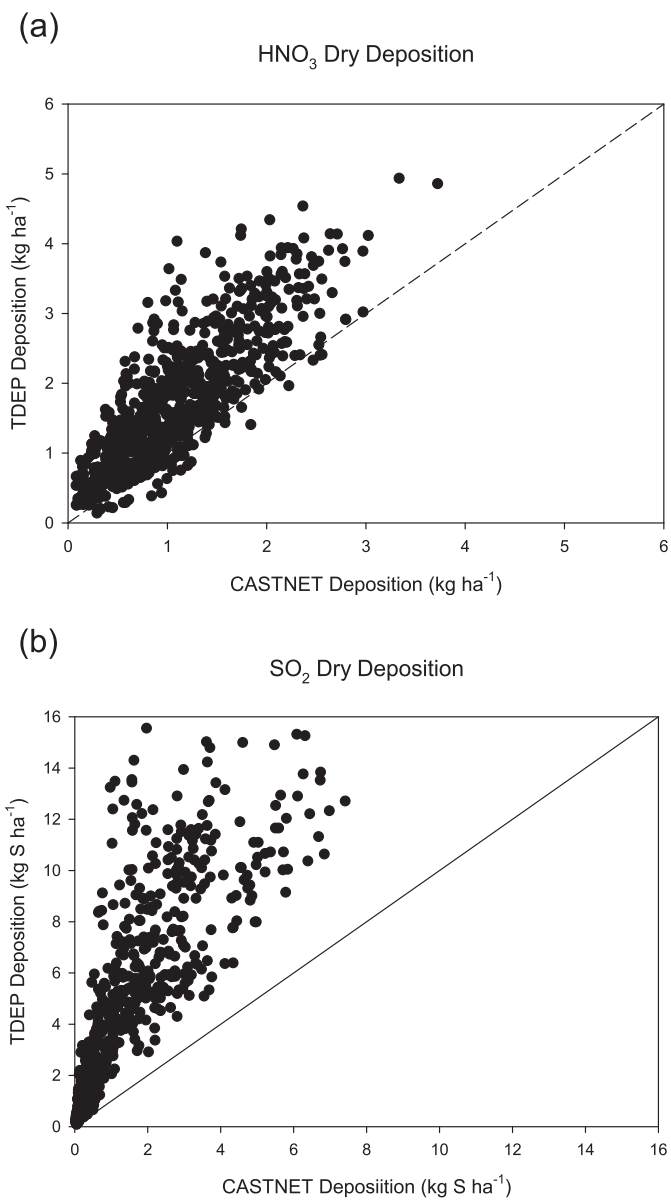

Fig. 10. Comparison of (a) HNO_3 and (b) SO_2 dry deposition (kg ha^{-1}) from the hybrid TDEP approach and CASTNET.

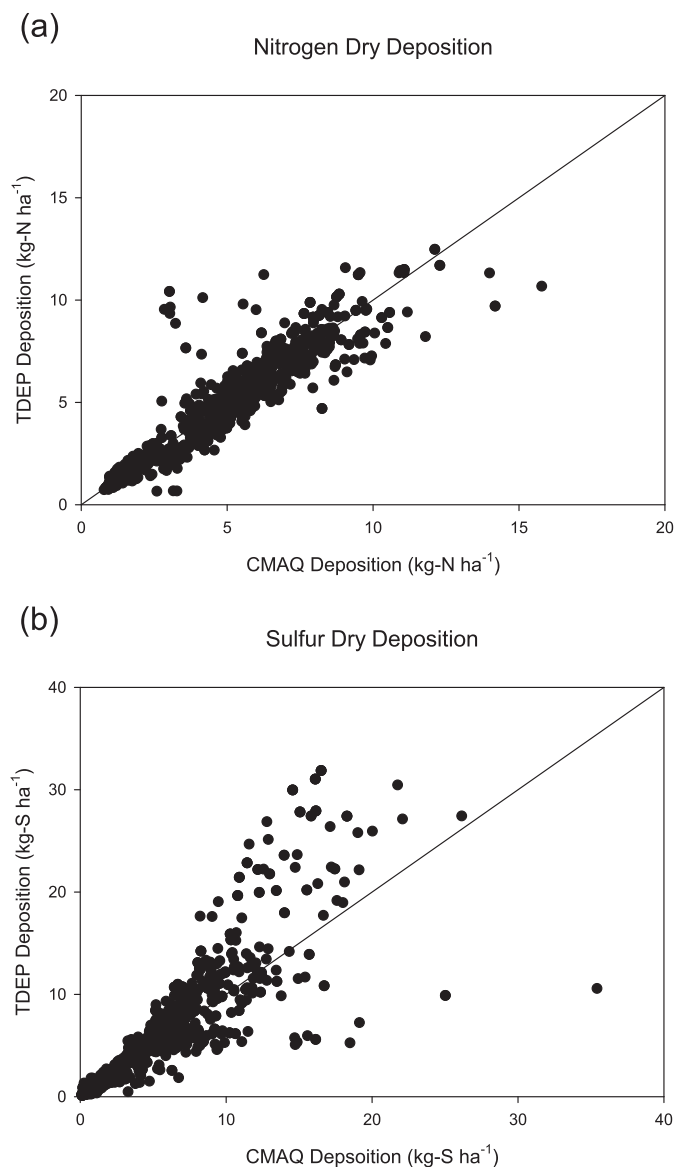

Fig. 11. Comparison of (a) nitrogen dry deposition (kg-N ha^{-1}) and sulfur dry deposition (kg-S ha^{-1}) from the hybrid TDEP approach and CMAQ.

(Fisher and Oppenheimer, 1991; Porter and Morris, 2005). Additionally, measurements of throughfall have been used to estimate total deposition. Without a substantial set of flux measurements, it is difficult to validate these various estimates, including the current hybrid methodology. Instead, we compared estimates from the hybrid approach with these other approaches for determining the total deposition. We provide a brief summary of some initial comparisons below. More complete analyses are ongoing.

First, we compared the dry deposition values from the hybrid approach with those from CASTNET. Since total deposition for CASTNET is derived using the same wet deposition as used in the hybrid approach, wet deposition was not included in this comparison. For most species, the deposition from the hybrid approach was higher than the values from CASTNET (Fig. 10). This is primarily due to the higher deposition velocities calculated by CMAQ compared to MLM. Differences in deposition velocity are driven by both the modeling approaches used in the models and the meteorological inputs. For example, the deposition of HNO_3, the major component of oxidized nitrogen deposition, is controlled by the aerodynamic resistance. In CMAQ, this key resistance is calculated based in Monin–Obukhov similarity theory while for CASTNET, MLM calculates the resistance based on an approximation using the standard deviation of the wind direction due to the instrumentation limitations at the sites. SO_2 deposition is often controlled by the cuticular resistance which is calculated in CMAQ based on Henry's Law to account for surface wetness resulting in quite low resistances. In contrast for CASTNET, the MLM sets a very high value for the cuticular resistance whether it is wet or dry. Further evaluation studies of deposition velocity algorithms are needed.

Next, we compared the values developed from the hybrid approach with those obtained from CMAQ alone. Meteorological models often struggle with correctly predicting precipitation amount and location. Therefore, we expect that wet deposition from CMAQ will be different than those from the hybrid approach since these the hybrid approach uses the PRISM adjusted values from NTN with CMAQ biases varying spatially and temporally. Dry deposition is calculated as the product of concentration and deposition velocity. So, the hybrid approach will produce different dry deposition values since the concentrations fields are not the same in the hybrid approach and CMAQ. A comparison of the nitrogen and sulfur dry deposition from CMAQ and the hybrid or TDEP approach is given in Fig. 11. There is overall good agreement between the deposition values for total nitrogen (Fig. 11a) while agreement for individual species such as HNO_3 and NH_3 is not as good (not shown). For sulfur deposition (Fig. 11b), the TDEP values

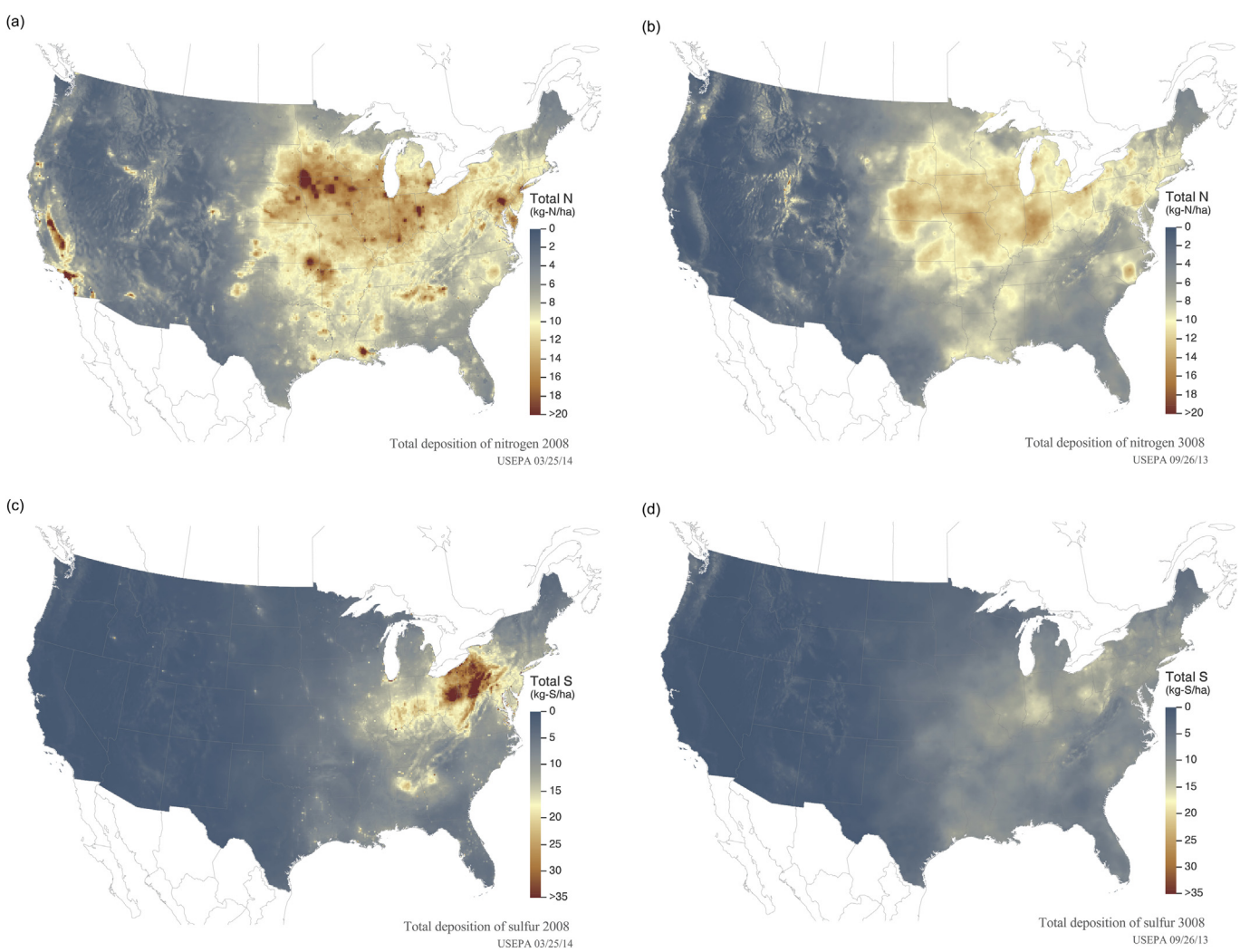

Fig. 12. Comparison of total (wet + dry) nitrogen deposition (kg-N ha^{-1}) for 2008 for (a) hybrid approach and (b) approximated as double the wet deposition. Comparison of total (wet + dry) sulfur deposition (kg-S ha^{-1}) for 2008 for (c) hybrid approach and (d) approximated as double the wet deposition.
Source: CASTNET/CMAQ/NTN/AMON/SEARCH.

Table 5
Comparison of total nitrogen deposition (kg-N ha^{-1}) and total sulfur deposition (kg-S ha^{-1}) for the hybrid TDEP method and throughfall (TFALL) for selected sites in the western U.S.

Year	Region	Latitude	Longitude	Total N deposition		Total S deposition	
				TDEP	TFALL	TDEP	TFALL
2007	WA	46.739	−121.816	2.626	0.470	1.545	
2007	WA	47.836	−123.981	3.749	0.940	2.582	
2008	C2CCRLAC	42.902	−122.279	6.873	0.500	1.469	
2008	CRG	45.816	−121.946	5.962	1.244	2.600	
2008	MBS	47.539	−121.573	4.452	2.762	3.165	
2008	Sierra	38.730	−120.550	6.811	3.049	1.017	
2008	Sierra	39.316	−120.849	7.099	7.176	1.065	
2008	Sierra	37.530	−119.670	6.581	3.271	1.197	
2008	WIL	44.213	−122.253	2.985	0.897	1.602	
2008	WIL	44.282	−122.034	2.692	0.626	1.446	
2011	Yosemite	37.819	−119.781	6.883	2.765	1.425	0.982
2011	Yosemite	37.526	−119.666	6.361	3.032	1.244	1.153
2011	Yosemite	37.759	−119.814	7.322	4.657	1.413	1.691
2011	Yosemite	37.802	−119.863	6.967	3.005	1.416	1.345
2011	Yosemite	37.855	−119.659	7.093	3.003	1.515	0.693
2011	Yosemite	37.712	−119.703	7.073	3.828	1.379	1.143
2011	Yosemite	37.734	−119.609	6.353	2.811	1.277	0.944

are substantially higher for some individual sites. These sites tend to be in the western U.S. where there are few network sites, but there are notable biases in the CMAQ values. The scarcity of sites influences the bias correction surface and points to the need to include additional monitoring networks such as IMPROVE in future versions.

As another comparison, we examined deposition estimates from the hybrid approach and those from the approximations of doubling the wet deposition. Since the processes that drive wet and dry deposition are quite different and the relative contributions of wet and dry deposition vary spatially and temporally, we would not expect the values to be the same. Fig. 12 provides a comparison of total deposition as determined by the hybrid method presented here with the estimate determined by doubling the wet deposition. Using only the wet deposition underestimates the strong contribution of local NH_3 sources as shown in Fig. 12a. Doubling the wet deposition results in estimates of sulfur deposition (Fig. 12b) in the northeast that are much lower than those predicted by the hybrid methodology.

Finally, we compared values from some throughfall studies (Fenn et al., 2010; Root et al., 2013) with those from the corresponding grid cells from the hybrid approach. A particular challenge with these studies is that the throughfall studies are ecosystem specific (e.g. forest) while the grid cell average may be dominated by a very different ecosystem (e.g. riparian). Therefore, we limited our comparisons to sites where the forested sites used for the throughfall measurements fell in a grid cell that was predominantly (>75%) forest. Throughfall and total deposition would not be expected to be equal since they represent different air–surface exchange processes, however we expect that throughfall would represent a lower limit of total deposition. A comparison of total deposition from the two methods for the selected sites followed this expected pattern (Table 5).

4. Conclusions

A hybrid methodology was developed to combine measured and modeled atmospheric concentration, deposition velocities, and deposition to create spatially continuous estimates of nitrogen and sulfur deposition for use in ecological analyses. The methodology is designed to give most weight to measured data and uses modeled data to fill in gaps in measurement data. Importantly, this methodology provides a time series of deposition from 2000 to 2012 which is needed as input to biogeochemical models. This data will be particularly useful to the water quality and ecological research communities.

Outputs from this effort are provided to the public via the CASTNET website. The data are provided as ESRI grid files and maps are provided as PNG files. The release described here is version 2014.v01 of the product which provides maps and data for 2000–2012. Updates will be released as new modeling and monitoring data become available and as the methodology is enhanced.

While this product represents an improvement over previous methods for determining spatially continuous total deposition for the US, future research in modeling and monitoring will be needed to improve estimates of deposition. For example, further work is needed in characterizing the sources and atmospheric chemistry of organic nitrogen compounds to improve monitoring and modeling capabilities. With the availability of bidirectional flux estimates for ammonia, appropriate methods for fusing observed data with the bidirectional flux will need to be developed. Improvements in the methodology can also be explored including investigating methods characterizing the mass balance issues, analyzing the sensitivity of the deposition values to interpolation methods, and exploring methods for addressing the artifacts introduced by non-continuous measurement data.

Acknowledgments

The authors wish to thank the NADP Total Deposition (TDEP) Steering Committee as well as TDEP meeting attendees for their many helpful suggestions on the development of this methodology. Additionally, we acknowledge helpful discussion with Kristen Foley, Robin Dennis and Prakash Bhave of EPA Atmospheric Modeling and Analysis Division. This project could not have been completed without the use of the data from the EPA CDC/PHASE study and we thank Wyat Appel, Sharon Philips, Alison Eyth and Eric Hall for making the data available to us. Finally, we wish to thank Mark Fenn for providing throughfall data for comparison with the values from the hybrid approach. The United States Environmental Protection Agency through its Office of Research and Development collaborated in the research described here. It has been subjected to Agency review and approved for publication.

Appendix A. Supplementary data

Supplementary data related to this article can be found at http://dx.doi.org/10.1016/j.atmosenv.2014.04.008.

References

Aber, J.D., Goodale, C.L., Ollinger, S.V., Smith, M.L., Magill, A.H., Martin, M.E., Hallett, R.A., Stoddard, J.L., 2003. Is nitrogen deposition altering the nitrogen status of northeastern forests? Bioscience 53, 375–389.

Anderson, D.M., Burkholder, J.M., Cochlan, W.P., Glibert, P.M., Gobler, C.J., Heil, C.A., Kudela, R.M., Parsons, M.L., Rensel, J.E.J., Townsend, D.W., Trainer, V.L., Vargo, G.A., 2008. Harmful algal blooms and eutrophication: examining linkages from selected coastal regions of the United States. Harmful Algae 8, 39–53.

Appel, K.W., Foley, K.M., Bash, J.O., Pinder, R.W., Dennis, R.L., Allen, D.J., Pickering, K., 2011. A multi-resolution assessment of the Community Multiscale Air Quality (CMAQ) model v4.7 wet deposition estimates for 2002–2006. Geoscience Model Development 4, 357–371.

Atmospheric Research and Analysis Inc (ARA), 2012. South Eastern Aerosol Research and Characterization (SEARCH) Network. http://www.atmospheric-research.com/public/index.html (accessed 07.07.12.).

Baumgardner, R.E., Lavery, T.F., Rogers, C.M., Isil, S.S., 2002. Estimates of the atmospheric deposition of sulfur and nitrogen Species: clean air status and trends network, 1990–2000. Environmental Science & Technology 36, 2614–2629.

Bobbink, R., Hicks, K., Galloway, J., Spranger, T., Alkemade, R., Ashmore, M., Bustamante, M., Cinderby, S., Davidson, E., Dentener, F., Emmett, B., Erisman, J.W., Fenn, M., Gilliam, F., Nordin, A., Pardo, L., De Vries, W., 2010. Global assessment of nitrogen deposition effects on terrestrial plant diversity: a synthesis. Ecological Applications 20, 30–59.

Byun, D., Schere, K.L., 2006. Review of the governing equations, computational algorithms, and other components of the Models-3 Community Multiscale Air Quality (CMAQ) modeling system. Applied Mechanics Reviews 59, 51–77.

Cape, J.N., Cornell, S.E., Jickells, T.D., Nemitz, E., 2011. Organic nitrogen in the atmosphere – where does it come from? A review of sources and methods. Atmospheric Research 102, 30–48.

Center for Disease Control and Prevention, 2013. National Environmental Health Tracking. http://www.cdc.gov/nceh/tracking/phase.htm (accessed 21.08.13.).

Colorado State University, 2014. Interagency Monitoring of Protected Visual Environments. http://vista.cira.colostate.edu/improve/Default.htm (accessed 27.03.14.).

Cornell, S.E., Jickells, T.D., Cape, J.N., Rowland, A.P., Duce, R.A., 2003. Organic nitrogen deposition on land and coastal environments: a review of methods and data. Atmospheric Environment 37, 2173–2191.

Cosby, B.J., Hornberger, G.M., Galloway, J.N., Wright, R.F., 1985. Modeling the effects of acid deposition: assessment of a lumped parameter model of soil water and stream water chemistry. Water Resources Research 21, 51–63.

Dennis, R.L., Foley, K.M., 2009. Adapting CMAQ Deposition Fields for Critical Loads Analyses, NADP Annual Meeting and Scientific Symposium. Saratoga Springs, (NY).

Driscoll, C.T., Lawrence, G.B., Bulger, A.J., Butler, T.J., Cronan, C.S., Eagar, C., Lambert, K.F., Likens, G.E., Stoddard, J.L., Weathers, K.C., 2001. Acidic deposition in the northeastern United States: sources and inputs, ecosystem effects, and management strategies. Bioscience 51, 180–198.

Driscoll, C.T., Whitall, D., Aber, J., Boyer, E., Castro, M., Cronan, C., Goodale, C.L., Groffman, P., Hopkinson, C., Lambert, K., Lawrence, G., Ollinger, S., 2003. Nitrogen pollution in the northeastern United States: sources, effects, and management options. Bioscience 53, 357–374.

Fenn, M.E., Allen, E.B., Weiss, S.B., Jovan, S., Geiser, L.H., Tonnesen, G.S., Johnson, R.F., Rao, L.E., Gimeno, B.S., Yuan, F., Meixner, T., Bytnerowicz, A., 2010. Nitrogen critical loads and management alternatives for N-impacted ecosystems in California. Journal of Environmental Management 91, 2404–2423.

Fenn, M.E., Baron, J.S., Allen, E.B., Rueth, H.M., Nydick, K.R., Geiser, L., Bowman, W.D., Sickman, J.O., Meixner, T., Johnson, D.W., Neitlich, P., 2003. Ecological effects of nitrogen deposition in the western United States. Bioscience 53, 404–420.

Fisher, D.C., Oppenheimer, M., 1991. Atmospheric nitrogen deposition and the Chesapeake Bay Estuary. Ambio 20, 102–108.

Foley, K.M., Roselle, S.J., Appel, K.W., Bhave, P.V., Pleim, J.E., Otte, T.L., Mathur, R., Sarwar, G., Young, J.O., Gilliam, R.C., Nolte, C.G., Kelly, J.T., Gilliland, A.B., Bash, J.O., 2010. Incremental testing of the Community Multiscale Air Quality (CMAQ) modeling system version 4.7. Geoscientific Model Development 3, 205–226.

Gbondo-Tugbawa, S.S., Driscoll, C.T., Aber, J.D., Likens, G.E., 2001. Evaluation of an integrated biogeochemical model (PnET-BGC) at a northern hardwood forest ecosystem. Water Resources Research 37, 1057–1070.

Grell, G., Dudhia, J., Stauffer, D., 1995. A Description of the Fifth-Generation Penn State/NCAR Mesoscale model (MM5). Boulder, CO. NCAR/TN-398+STR.

Hall, E.S., Eyth, A.M., Phillips, S.B., 2012a. Hierarchical Bayesian Model (HBM) – Derived Estimates of Air Quality for 2007: Annual Report. U.S. Environmental Protection Agency, Washington, DC, p. 300.

Hall, E.S., Eyth, A.M., Phillips, S.B., 2012b. Hierarchical Bayesian Model (HBM) – Derived Estimates of Air Quality for 2008: Annual Report. U.S. Environmental Protection Agency, Washington, DC, p. 192.

Heisler, J., Glibert, P.M., Burkholder, J.M., Anderson, D.M., Cochlan, W., Dennison, W.C., Dortch, Q., Gobler, C.J., Heil, C.A., Humphries, E., 2008. Eutrophication and harmful algal blooms: a scientific consensus. Harmful algae 8, 3–13.

Howarth, R., 2008. Estimating atmospheric nitrogen deposition in the northeastern United States: relevance to Narragansett Bay. In: Desbonnet, A., Costa-Pierce, B.A. (Eds.), Science for Ecosystem-based Management: Narragansett Bay in the 21st Century. Springer, pp. 43–61.

Meyers, T.P., Finkelstein, P., Clarke, J., Ellestad, T.G., Sims, P.F., 1998. A multilayer model for inferring dry deposition using standard meteorological measurements. Journal of Geophysical Research 103, 22645–22661.

National Atmospheric Deposition Program, 2012. National Trends Network. http://nadp.sws.uiuc.edu/NTN/ntnData.aspx (accessed 10.10.12.).

Neff, J.C., Holland, E.A., Dentener, F., McDowell, W.H., Russell, K.M., 2002. The origin, composition and rates of organic nitrogen deposition: a missing piece of the nitrogen cycle? Biogeochemistry 57-58, 99–136.

Paerl, H., Dennis, R., Whitall, D., 2002. Atmospheric deposition of nitrogen: implications for nutrient over-enrichment of coastal waters. Estuaries 25, 677–693.

Paerl, H.W., Whithall, D.R., 1999. Anthropogenically-derived atmospheric nitrogen deposition, marine eutrophication, and harmful algal bloom expansion: is there a link? Ambio 28, 307–311.

Pardo, L.H., Fenn, M.E., Goodale, C.L., Geiser, L.H., Driscoll, C.T., Allen, E.B., Baron, J.S., Bobbink, R., Bowman, W.D., Clark, C.M., 2011. Effects of nitrogen deposition and empirical nitrogen critical loads for ecoregions of the United States. Ecological Applications 21, 3049–3082.

Perring, A.E., Pusede, S.E., Cohen, R.C., 2013. An observational perspective on the atmospheric impacts of alkyl and multifunctional nitrates on ozone and secondary organic aerosol. Chemical Reviews 113, 5848–5870.

Porter, E., Morris, K., 2005. Wet Deposition Monitoring Protocol for the National Park Service. National Park Service, US Department of the Interior, Washington, DC. D-1655.

PRISM Climate Group (PRISM), 2012. PRISM Climate Group (PRISM). Oregon State University. http://www.prism.oregonstate.edu/ (accessed 24.07.12.).

Root, H.T., Geiser, L.H., Fenn, M.E., Jovan, S., Hutten, M.A., Ahuja, S., Dillman, K., Schirokauer, D., Berryman, S., McMurray, J.A., 2013. A simple tool for estimating throughfall nitrogen deposition in forests of western North America using lichens. Forest Ecology and Management 306, 1–8.

Skamarock, W., Klemp, J., Dudhia, J., Gill, D., Barker, D., Wang, W., Huang, X.-y., Duda, M., 2008. A Description of the Advanced Research WRF Version 3. University Corporation for Atmospheric Research. NCAR Tech. Note NCAR/TN-475+STR.

Turnipseed, A.A., Huey, L.G., Nemitz, E., Stickel, R., Higgs, J., Tanner, D.J., Slusher, D.L., Sparks, J.P., Flocke, F., Guenther, A., 2006. Eddy covariance fluxes of peroxyacetyl nitrates (PANs) and NOy to a coniferous forest. Journal of Geophysical Research 111, D09304.

U.S. Environmental Protection Agency, 2013a. Bayesian Space-time Downscaling Fusion Model (Downscaler) – Derived Estimates of Air Quality for 2009. U.S. Environmental Protection Agency, Washington, DC.

U.S. Environmental Protection Agency, 2013b. Clean Air Act. http://www.epa.gov/oar/caa/caa112.txt (accessed 27.03.14.).

U.S. Environmental Protection Agency, 2013c. The Clean Air Status and Trends Network (CASTNET). http://www.epa.gov/castnet (accessed 13.06.13.).

U.S. Environmental Protection Agency, 2014. Technology Transfer Network/NAAQS Ozone Implementation. http://www.epa.gov/ttn/naaqs/ozone/rto/sip/related.html#final (accessed 27.03.14.).

UNC, 2013. SMOKE – Sparse Matrix Operator Kernel Emissions. http://www.smoke-model.org/index.cfm (accessed 5.03.13.).

Vitousek, P.M., Aber, J.D., Howarth, R.W., Likens, G.E., Matson, P.A., Schindler, D.W., Schlesinger, W.H., Tilman, D.G., 1997. Human alteration of the global nitrogen cycle: sources and consequences. Ecological Applications 7, 737–750.

Xing, J., Pleim, J., Mathur, R., Pouliot, G., Hogrefe, C., Gan, C.M., Wei, C., 2013. Historical gaseous and primary aerosol emissions in the United States from 1990 to 2010. Atmospheric Chemistry and Physics 13, 7531–7549.

Supplemental Information

Table 1. Locations of network sites and years of operation used in the hybrid methodology.

NETWORK	SITE ID	SITE NAME	START DATE	END DATE
AMON	AL99	Sand Mountain Research & Extension Center	3/29/2011	
AMON	AR03	Caddo Valley	3/1/2011	
AMON	AZ98	Chiricahua	3/15/2011	
AMON	CA44		3/15/2011	
AMON	CA67	Joshua Tree National Park-Black Rock	3/1/2011	
AMON	CA83		3/22/2011	
AMON	CO13	Fort Collins	11/27/2007	
AMON	CO88	Rocky Mountain National Park - Longs Peak	5/10/2011	
AMON	CO98	Rocky Mountain National Park-Loch Vale	5/10/2011	
AMON	CT15	Abington	3/29/2011	
AMON	FL11	Everglades National Park-Research Center	3/15/2011	
AMON	FL19	Indian River	4/26/2011	
AMON	GA40	Yorkville	12/23/2011	
AMON	GA41	Georgia Station	6/7/2011	
AMON	ID03	Craters of the Moon National Monument	6/7/2010	
AMON	IL11	Bondville	10/30/2007	
AMON	IL37		4/26/2011	
AMON	IL46	Alhambra	3/3/2011	
AMON	IN99	Indianapolis	10/30/2007	
AMON	KS03	Reserve	10/11/2011	
AMON	KS31	Konza Prairie	3/1/2011	
AMON	KS98	Coffeyville	10/30/2007	4/26/2011
AMON	KY03	Mackville	3/1/2011	
AMON	KY98	Cadiz	3/15/2011	
AMON	MD08	Piney Reservoir	8/3/2010	
AMON	MD99	Beltsville	8/3/2010	
AMON	MI96	Detroit	10/29/2007	
AMON	MN18	Fernberg	10/30/2007	
AMON	MN29	Blue Mounds	10/30/2007	3/3/2009
AMON	MN42	Great River Bluffs	10/30/2007	3/10/2009
AMON	NC06	Beaufort	4/27/2010	
AMON	NC25	Coweeta	5/24/2011	
AMON	NC26	Candor	4/26/2011	
AMON	NC30	Duke Forest	6/24/2008	
AMON	NC35	Clinton Crops Research Station	11/25/2008	2/10/2010
AMON	NC99	Durham	6/24/2008	2/11/2009
AMON	NE98	Santee	4/26/2011	
AMON	NJ98		3/1/2011	
AMON	NM98	Navajo Lake	1/11/2008	
AMON	NM99	Farmington	1/9/2008	

AMON	NY16	Millbrook	10/13/2009	
AMON	NY67	Ithaca	10/30/2007	
AMON	OH02	Athens Super Site	10/30/2007	
AMON	OH27	Cincinnati	10/30/2007	
AMON	OH54	Deer Creek State Park	3/1/2011	
AMON	OK99	Stilwell	10/30/2007	
AMON	ON07	Egbert	10/30/2007	12/21/2010
AMON	PA00	Arendtsville	10/13/2009	
AMON	PA29	Kane Experimental Forest	3/8/2011	
AMON	SC05	Cape Romain National Wildlife Refuge	10/30/2007	
AMON	TN01		3/15/2011	
AMON	TX43	Cañónceta	10/30/2007	
AMON	UT01	Logan	11/8/2011	
AMON	UT97	Salt Lake City	11/8/2011	
AMON	VA24	Prince Edward	3/1/2011	
AMON	WA99	Mount Rainier National Park-Tahoma Woods	3/16/2011	
AMON	WI07	Mayville	10/30/2007	
AMON	WI35	Perkinstown	3/29/2011	
AMON	WV18	Parsons	6/7/2011	
AMON	WY94	Grand Tetons National Park	9/22/2011	
CASTNET	ABT147	Abington	12/21/1993	
CASTNET	ACA416	Acadia NP	2/1/1998	
CASTNET	ALC188	Alabama-Coushatta	4/2/2004	
CASTNET	ALH157	Alhambra	5/12/1988	
CASTNET	ANA115	Ann Arbor	4/14/1988	
CASTNET	ARE128	Arendtsville	5/21/1988	
CASTNET	ASH135	Ashland	12/18/1988	
CASTNET	BBE401	Big Bend NP	7/1/1995	
CASTNET	BEL116	Beltsville	10/25/1988	
CASTNET	BFT142	Beaufort	12/28/1993	
CASTNET	BVL130	Bondville	2/1/1988	
CASTNET	BWR139	Blackwater NWR	7/4/1995	
CASTNET	CAD150	Caddo Valley	9/28/1988	
CASTNET	CAN407	Canyonlands NP	1/1/1995	
CASTNET	CAT175	Claryville	5/1/1994	
CASTNET	CDR119	Cedar Creek	11/7/1987	
CASTNET	CDZ171	Cadiz	9/28/1993	
CASTNET	CHA467	Chiricahua NM	4/22/1989	
CASTNET	CHE185	Cherokee Nation	4/2/2002	
CASTNET	CKT136	Crockett	8/24/1993	
CASTNET	CND125	Candor	9/20/1990	
CASTNET	CNT169	Centennial	5/9/1989	
CASTNET	CON186	Converse Station	6/17/2003	1/31/2011
CASTNET	COW137	Coweeta	11/1/1987	
CASTNET	CTH110	Connecticut Hill	8/21/1987	
CASTNET	CVL151	Coffeeville	10/1/1988	
CASTNET	DCP114	Deer Creek	9/14/1988	

CASTNET	DEN417	Denali NP	1/1/1998	
CASTNET	DEV412	Death Valley NM	1/1/1995	12/31/2007
CASTNET	EGB181	Egbert	7/17/1994	
CASTNET	ESP127	Edgar Evins	3/15/1988	
CASTNET	EVE419	Everglades NP	1/1/1998	
CASTNET	GAS153	Georgia Station	4/21/1988	
CASTNET	GLR468	Glacier NP	10/12/1988	
CASTNET	GRB411	Great Basin NP	4/1/1995	
CASTNET	GRC474	Grand Canyon NP	5/16/1989	
CASTNET	GRS420	Great Smoky NP - Look Rock	1/1/1998	
CASTNET	GTH161	Gothic	5/13/1989	
CASTNET	HOW132	Howland	11/24/1992	
CASTNET	HOW191	Howland Ameriflux	9/16/2011	
CASTNET	HOX148	Hoxeyville	10/28/2000	
CASTNET	HVT424	Hawaii Volcanoes NP	8/3/1999	7/17/2004
CASTNET	HWF187	Huntington Wildlife Forest	5/28/2002	
CASTNET	IRL141	Indian River Lagoon	7/8/2001	
CASTNET	JOT403	Joshua Tree NP	2/1/1995	
CASTNET	KEF112	Kane Exp. Forest	12/19/1988	
CASTNET	KNZ184	Konza Prairie	3/26/2002	
CASTNET	KVA428	Kobuk Valley NP	5/18/2004	9/30/2005
CASTNET	LAV410	Lassen Volcanic NP	7/1/1995	
CASTNET	LRL117	Laurel Hill	12/11/1987	
CASTNET	LYE145	Lye Brook	10/23/1993	3/31/2007
CASTNET	LYK123	Lykens	9/14/1988	10/13/2010
CASTNET	MAC426	Mammoth Cave NP	7/24/2002	
CASTNET	MCK131	Mackville	7/30/1990	
CASTNET	MEV405	Mesa Verde NP	1/1/1995	
CASTNET	MKG113	M.K. Goddard	1/8/1988	
CASTNET	MOR409	Mount Rainier NP	8/1/1995	
CASTNET	NCS415	North Cascades NP	2/1/1996	12/31/2007
CASTNET	OLY421	Olympic NP	10/6/1998	2/28/2005
CASTNET	OXF122	Oxford	8/17/1987	
CASTNET	PAL190	Palo Duro	4/24/2007	
CASTNET	PAR107	Parsons	1/4/1988	
CASTNET	PED108	Prince Edward	10/29/1987	
CASTNET	PET427	Petrified Forest	9/12/2002	
CASTNET	PIN414	Pinnacles NM	5/1/1995	
CASTNET	PND165	Pinedale	10/21/1988	
CASTNET	PNF126	Cranberry	9/24/1988	
CASTNET	POF425	Poker Flats, Yukon Flats NM	7/1/2001	2/29/2004
CASTNET	PRK134	Perkinstown	9/17/1988	
CASTNET	PSU106	Penn State	1/1/1987	
CASTNET	QAK172	Quaker City	7/28/1993	
CASTNET	ROM406	Rocky Mtn NP	10/1/1994	
CASTNET	RTP101	Res. Triangle Pk.	1/1/1987	11/28/2006
CASTNET	SAL133	Salamonie Reservoir	5/3/1988	

CASTNET	SAN189	Santee Sioux	7/5/2006	
CASTNET	SEK402	Sequoia NP - Lookout Pt	2/1/1997	2/22/2005
CASTNET	SEK430	Sequoia NP - Ash Mountain	4/1/2005	
CASTNET	SHN418	Shenandoah NP - Big Meadows	5/17/1988	
CASTNET	SND152	Sand Mountain	11/17/1988	
CASTNET	SPD111	Speedwell	6/9/1989	
CASTNET	STK138	Stockton	12/14/1993	
CASTNET	SUM156	Sumatra	12/27/1988	
CASTNET	THR422	Theodore Roosevelt NP	8/1/1998	
CASTNET	UVL124	Unionville	5/20/1988	
CASTNET	VII423	Virgin Islands NP - Lind Pt	4/1/1998	1/31/2004
CASTNET	VIN140	Vincennes	6/18/1987	
CASTNET	VOY413	Voyageurs NP	6/1/1996	
CASTNET	VPI120	Horton Station	5/1/1987	
CASTNET	WFM105	Whiteface Mountain	1/1/1987	
CASTNET	WNC429	Wind Cave NP	11/1/2003	
CASTNET	WSP144	Wash. Crossing	12/1/1988	
CASTNET	WST109	Woodstock	12/21/1988	
CASTNET	YEL408	Yellowstone NP	6/1/1996	
CASTNET	YOS404	Yosemite NP - Turtleback Dome	9/25/1995	
NTN	AK01	Poker Creek	12/29/1992	
NTN	AK02	Juneau	6/22/2004	
NTN	AK03	Denali National Park-Mt. McKinley	6/17/1980	
NTN	AK06	Gates of the Arctic National Park - Bettles	11/4/2008	
NTN	AK97	Katmai National Park - King Salmon	11/2/2009	
NTN	AK99	Ambler	5/12/2004	8/9/2005
NTN	AL02	Delta Elementary	6/5/2001	12/31/2009
NTN	AL02	Delta Elementary	6/5/2001	1/5/2010
NTN	AL03	Centreville	6/20/2000	
NTN	AL10	Black Belt Research & Extension Center	8/31/1983	
NTN	AL24	Bay Road	5/22/2001	12/31/2009
NTN	AL24	Bay Road	5/29/2001	1/5/2010
NTN	AL99	Sand Mountain Research & Extension Center	10/2/1984	
NTN	AR02	Warren 2WSW	5/25/1982	
NTN	AR03	Caddo Valley	12/30/1983	
NTN	AR03	Caddo Valley	3/1/2011	
NTN	AR16	Buffalo National River-Buffalo Point	7/13/1982	
NTN	AR27	Fayetteville	5/13/1980	
NTN	AZ03	Grand Canyon National Park-Hopi Point	8/11/1981	
NTN	AZ06	Organ Pipe Cactus National Monument	4/15/1980	
NTN	AZ97	Petrified Forest National Park-Rainbow Forest	12/3/2002	
NTN	AZ98	Chiricahua	2/23/1999	
NTN	AZ99	Oliver Knoll	8/25/1981	
NTN	CA28	Kings River Experimental Watershed	4/24/2007	
NTN	CA42	Tanbark Flat	1/12/1982	
NTN	CA45	Hopland	10/3/1979	
NTN	CA50	Sagehen Creek	11/6/2001	

NTN	CA66	Pinnacles National Monument-Bear Valley	11/2/1999	
NTN	CA67	Joshua Tree National Park-Black Rock	9/19/2000	
NTN	CA67	Joshua Tree National Park-Black Rock	3/1/2011	
NTN	CA75	Sequoia National Park-Giant Forest	7/8/1980	
NTN	CA75	Sequoia National Park-Giant Forest	7/22/2003	
NTN	CA76	Montague	6/25/1985	
NTN	CA88	Davis	9/4/1978	
NTN	CA94	Converse Flats	4/20/2006	
NTN	CA94	Converse Flats	5/9/2006	
NTN	CA95	Death Valley National Park-Cow Creek	2/8/2000	5/31/2005
NTN	CA96	Lassen Volcanic National Park-Manzanita Lake	6/13/2000	
NTN	CA99	Yosemite National Park-Hodgdon Meadow	12/8/1981	
NTN	CO00	Alamosa	4/22/1980	
NTN	CO01	Las Animas Fish Hatchery	10/4/1983	
NTN	CO02	Niwot Saddle	6/5/1984	
NTN	CO08	Four Mile Park	12/29/1987	
NTN	CO10	Gothic	2/2/1999	
NTN	CO15	Sand Spring	3/20/1979	
NTN	CO18	Ripple Creek Pass	5/13/2003	1/13/2009
NTN	CO19	Rocky Mountain National Park-Beaver Meadows	5/29/1980	
NTN	CO21	Manitou	10/17/1978	
NTN	CO22	Pawnee	5/22/1979	
NTN	CO89	Rocky Mountain National Park-Loch Vale	9/29/2009	
NTN	CO90	Niwot Ridge-Southeast	1/24/2006	
NTN	CO91	Wolf Creek Pass	5/26/1992	
NTN	CO92	Sunlight Peak	1/13/1988	
NTN	CO93	Buffalo Pass - Dry Lake	10/14/1986	
NTN	CO94	Sugarloaf	11/4/1986	
NTN	CO96	Molas Pass	7/29/1986	
NTN	CO96	Molas Pass	6/30/2009	
NTN	CO97	Buffalo Pass - Summit Lake	2/7/1984	
NTN	CO97	Buffalo Pass - Summit Lake	9/29/1998	
NTN	CO98	Rocky Mountain National Park-Loch Vale	8/16/1983	
NTN	CO99	Mesa Verde National Park-Chapin Mesa	4/28/1981	
NTN	CO99	Mesa Verde National Park-Chapin Mesa	12/26/2001	
NTN	CT15	Abington	1/26/1999	
NTN	DE99	Trap Pond State Park	5/30/2001	5/26/2003
NTN	DE99	Trap Pond State Park	5/27/2003	9/23/2008
NTN	FL03	Bradford Forest	10/10/1978	
NTN	FL05	Chassahowitzka National Wildlife Refuge	8/27/1996	
NTN	FL05	Chassahowitzka National Wildlife Refuge	7/1/1997	
NTN	FL11	Everglades National Park-Research Center	6/17/1980	
NTN	FL11	Everglades National Park-Research Center	3/5/1996	
NTN	FL14	Quincy	3/13/1984	
NTN	FL23	Sumatra	1/26/1999	
NTN	FL32	Orlando	9/5/2003	9/25/2007

NTN	FL32	Orlando	12/14/2005	
NTN	FL41	Verna Well Field	8/25/1983	
NTN	FL99	Kennedy Space Center	8/2/1983	
NTN	GA09	Okefenokee National Wildlife Refuge	6/3/1997	
NTN	GA09	Okefenokee National Wildlife Refuge	7/29/1997	
NTN	GA20	Bellville	4/26/1983	
NTN	GA33	Sapelo Island	11/26/2002	
NTN	GA33	Sapelo Island	9/25/2007	
NTN	GA41	Georgia Station	10/3/1978	
NTN	GA98	Skidaway	6/18/2002	5/24/2005
NTN	GA99	Chula	2/10/1994	
NTN	HI99	Hawaii Volcanoes National Park-Thurston	11/21/2000	2/15/2005
NTN	IA08	Big Springs Fish Hatchery	8/14/1984	
NTN	IA23	McNay Research Center	9/11/1984	
NTN	ID02	Priest River Experimental Forest	12/31/2002	
NTN	ID03	Craters of the Moon National Monument	8/22/1980	
NTN	ID03	Craters of the Moon National Monument	10/21/2006	
NTN	ID03	Craters of the Moon National Monument	6/7/2010	
NTN	ID11	Reynolds Creek	11/22/1983	
NTN	ID15	Smiths Ferry	10/9/1984	9/27/2006
NTN	IL11	Bondville	2/27/1979	
NTN	IL11	Bondville	10/1/1992	
NTN	IL11	Bondville	1/6/1999	
NTN	IL11	Bondville	10/30/2007	
NTN	IL18	Shabbona	5/26/1981	
NTN	IL19	Argonne	3/11/1980	9/28/2004
NTN	IL46	Alhambra	1/26/1999	
NTN	IL46	Alhambra	3/1/2011	
NTN	IL63	Dixon Springs Agricultural Center	1/30/1979	
NTN	IL78	Monmouth	1/8/1985	
NTN	IN20	Roush Lake	8/22/1983	
NTN	IN20	Roush Lake	10/26/2000	1/26/2010
NTN	IN22	Southwest Purdue Agriculture Center	9/25/1984	
NTN	IN34	Indiana Dunes National Lakeshore	7/15/1980	
NTN	IN34	Indiana Dunes National Lakeshore	10/27/2000	
NTN	IN41	Agronomy Center for Research and Extension	7/13/1982	
NTN	KS07	Farlington Fish Hatchery	3/27/1984	
NTN	KS31	Konza Prairie	8/17/1982	
NTN	KS31	Konza Prairie	3/1/2011	
NTN	KS32	Lake Scott State Park	3/27/1984	
NTN	KS32	Lake Scott State Park	6/10/2008	
NTN	KY03	Mackville	11/29/1983	
NTN	KY03	Mackville	3/1/2011	
NTN	KY10	Mammoth Cave National Park-Houchin Meadow	8/27/2002	
NTN	KY19	Seneca Park	10/7/2003	
NTN	KY22	Lilley Cornett Woods	9/6/1983	
NTN	KY35	Clark State Fish Hatchery	8/30/1983	

NTN	KY99	Mulberry Flat	12/27/1994	
NTN	LA12	Iberia Research Station	11/16/1982	7/27/2010
NTN	LA30	Southeast Research Station	1/18/1983	
NTN	MA01	North Atlantic Coastal Lab	12/15/1981	
NTN	MA01	North Atlantic Coastal Lab	7/29/2003	
NTN	MA08	Quabbin Reservoir	3/5/1982	
NTN	MA13	East	2/2/1982	9/28/2010
NTN	MD03	White Rock Substation	10/3/1984	3/4/2002
NTN	MD07	Catoctin Mountain Park	5/27/2003	
NTN	MD08	Piney Reservoir	6/29/2004	
NTN	MD08	Piney Reservoir	1/1/2008	
NTN	MD08	Piney Reservoir	8/3/2010	
NTN	MD13	Wye	3/8/1983	
NTN	MD15	Smith Island	11/17/1995	6/1/2004
NTN	MD15	Smith Island	6/1/2004	
NTN	MD18	Assateague Island National Seashore-Woodcock	9/5/2000	
NTN	MD99	Beltsville	6/1/2004	
NTN	MD99	Beltsville	11/7/2006	
NTN	MD99	Beltsville	8/3/2010	
NTN	ME00	Caribou	4/14/1980	
NTN	ME00	Caribou	5/9/2007	
NTN	ME02	Bridgton	9/30/1980	
NTN	ME02	Bridgton	6/3/1997	
NTN	ME04	Carrabassett Valley	3/12/2002	
NTN	ME04	Carrabassett Valley	2/17/2009	
NTN	ME08	Gilead	9/28/1999	
NTN	ME09	Greenville Station	11/20/1979	
NTN	ME09	Greenville Station	9/3/1996	
NTN	ME95	Wolapomomqot Ciw Wocuk	6/12/2002	12/12/2006
NTN	ME95	Wolapomomqot Ciw Wocuk	10/4/2005	12/12/2006
NTN	ME96	Casco Bay-Wolfe’s Neck Farm	1/6/1998	
NTN	ME98	Acadia National Park-McFarland Hill	11/3/1981	
NTN	ME98	Acadia National Park-McFarland Hill	3/5/1996	
NTN	MI09	Douglas Lake	7/3/1979	
NTN	MI26	Kellogg Biological Station	6/26/1979	
NTN	MI29	Peshawbestown	1/22/2002	3/31/2009
NTN	MI29	Peshawbestown	5/8/2007	9/1/2009
NTN	MI48	Seney National Wildlife Refuge-Headquarters	11/28/2000	
NTN	MI48	Seney National Wildlife Refuge-Headquarters	11/11/2003	
NTN	MI51	Unionville	1/26/1999	
NTN	MI52	Ann Arbor	1/26/1999	
NTN	MI53	Wellston	10/10/1978	
NTN	MI97	Isle Royale National Park-Wallace Lake	5/22/1985	10/10/2006
NTN	MI98	Raco	5/1/1984	
NTN	MI99	Chassell	2/15/1983	
NTN	MN01	Cedar Creek	12/31/1996	

NTN	MN05	Fond du Lac	11/19/1996	3/22/2005
NTN	MN08	Hovland	12/31/1996	
NTN	MN16	Marcell Experimental Forest	7/6/1978	
NTN	MN16	Marcell Experimental Forest	2/27/1996	
NTN	MN18	Fernberg	11/18/1980	
NTN	MN18	Fernberg	3/5/1996	
NTN	MN18	Fernberg	10/30/2007	
NTN	MN23	Camp Ripley	10/18/1983	
NTN	MN23	Camp Ripley	7/2/1996	
NTN	MN27	Lamberton	1/2/1979	
NTN	MN27	Lamberton	7/2/1996	
NTN	MN28	Grindstone Lake	12/31/1996	
NTN	MN32	Voyageurs National Park-Sullivan Bay	5/30/2000	
NTN	MN99	Wolf Ridge	12/31/1996	
NTN	MO03	Ashland Wildlife Area	10/20/1981	
NTN	MO03	Ashland Wildlife Area	7/13/2010	
NTN	MO05	University Forest	10/27/1981	
NTN	MO43	Tyson Research Center	8/28/2001	5/7/2008
NTN	MS10	Clinton	7/10/1984	
NTN	MS12	Grand Bay NERR	9/29/2006	
NTN	MS12	Grand Bay NERR	3/9/2010	
NTN	MS19	Newton	11/11/1986	
NTN	MS30	Coffeeville	7/17/1984	
NTN	MT00	Little Bighorn Battlefield National Monument	7/13/1984	
NTN	MT05	Glacier National Park-Fire Weather Station	6/3/1980	
NTN	MT05	Glacier National Park-Fire Weather Station	10/28/2003	
NTN	MT07	Clancy	1/24/1984	
NTN	MT96	Poplar River	12/21/1999	
NTN	MT97	Lost Trail Pass	9/25/1990	
NTN	MT98	Havre - Northern Agricultural Research Center	7/30/1985	
NTN	NC03	Lewiston	10/31/1978	
NTN	NC06	Beaufort	1/26/1999	
NTN	NC06	Beaufort	4/27/2010	
NTN	NC25	Coweeta	7/5/1978	
NTN	NC29	Hofmann Forest	7/2/2002	
NTN	NC34	Piedmont Research Station	10/17/1978	
NTN	NC35	Clinton Crops Research Station	10/24/1978	
NTN	NC35	Clinton Crops Research Station	8/5/2008	2/16/2010
NTN	NC36	Jordan Creek	10/18/1983	
NTN	NC41	Finley Farm	10/3/1978	
NTN	NC45	Mt. Mitchell	11/26/1985	
NTN	ND00	Theodore Roosevelt National Park-Painted Canyon	1/30/2001	
NTN	ND08	Icelandic State Park	10/25/1983	
NTN	ND11	Woodworth	11/29/1983	
NTN	NE15	Mead	7/25/1978	
NTN	NE15	Mead	6/26/2007	

NTN	NE99	North Platte Agricultural Experiment Station	9/24/1985	
NTN	NE99	North Platte Agricultural Experiment Station	10/14/2008	9/28/2010
NTN	NH02	Hubbard Brook	7/25/1978	
NTN	NH02	Hubbard Brook	2/3/2004	2/8/2005
NTN	NJ00	Edwin B. Forsythe National Wildlife Refuge	10/13/1998	
NTN	NJ99	Washington Crossing	8/4/1981	
NTN	NJ99	Washington Crossing	3/1/2011	
NTN	NM01	Gila Cliff Dwellings National Monument	7/29/1985	
NTN	NM07	Bandelier National Monument	6/22/1982	
NTN	NM08	Mayhill	1/24/1984	
NTN	NM12	Capulin Volcano National Monument	11/15/1984	
NTN	NV00	Red Rock Canyon	1/22/1985	12/10/2002
NTN	NV03	Smith Valley	8/7/1985	
NTN	NV05	Great Basin National Park-Lehman Caves	1/15/1985	
NTN	NY01	Alfred	8/17/2004	
NTN	NY08	Aurora Research Farm	4/17/1979	
NTN	NY10	Chautauqua	6/10/1980	
NTN	NY20	Huntington Wildlife	10/31/1978	
NTN	NY20	Huntington Wildlife	12/10/1999	
NTN	NY20	Huntington Wildlife	11/21/2007	
NTN	NY22	Akwesasne Mohawk-Fort Covington	8/18/1999	
NTN	NY29	Moss Lake	7/29/2003	
NTN	NY52	Bennett Bridge	6/10/1980	
NTN	NY65	Jasper	2/19/1980	6/15/2004
NTN	NY68	Biscuit Brook	10/11/1983	
NTN	NY68	Biscuit Brook	3/9/2004	
NTN	NY96	Cedar Beach, Southold	11/25/2003	
NTN	NY98	Whiteface Mountain	7/3/1984	
NTN	NY99	West Point	9/13/1983	
NTN	NY99	West Point	10/31/2006	10/26/2010
NTN	OH09	Oxford	8/14/1984	
NTN	OH15	Lykens	1/26/1999	10/12/2010
NTN	OH17	Delaware	10/3/1978	
NTN	OH49	Caldwell	9/26/1978	
NTN	OH54	Deer Creek State Park	1/26/1999	
NTN	OH54	Deer Creek State Park	3/1/2011	
NTN	OH71	Wooster	9/26/1978	
NTN	OK00	Salt Plains National Wildlife Refuge	12/13/1983	
NTN	OK08	Lake Eucha	2/1/2000	1/28/2004
NTN	OK17	Kessler Farm Field Laboratory	3/29/1983	
NTN	OK29	Goodwell Research Station	1/8/1985	
NTN	OK99	Stilwell	4/29/2003	
NTN	OK99	Stilwell	5/22/2007	7/28/2009
NTN	OK99	Stilwell	10/30/2007	
NTN	OK99	Stilwell	10/20/2008	
NTN	OR02	Alsea Guard Ranger Station	12/27/1979	12/26/2007
NTN	OR09	Silver Lake Ranger Station	8/23/1983	

NTN	OR10	H. J. Andrews Experimental Forest	5/13/1980	
NTN	OR10	H. J. Andrews Experimental Forest	12/13/2002	1/4/2011
NTN	OR18	Starkey Experimental Forest	3/6/1984	
NTN	OR97	Hyslop Farm	4/26/1983	
NTN	OR98	Bull Run	7/13/1982	10/6/2003
NTN	PA00	Arendtsville	1/26/1999	
NTN	PA00	Arendtsville	11/14/2000	
NTN	PA00	Arendtsville	10/13/2009	
NTN	PA15	Penn State	6/7/1983	
NTN	PA15	Penn State	10/6/1992	
NTN	PA18	Young Woman's Creek	4/20/1999	
NTN	PA29	Kane Experimental Forest	7/18/1978	
NTN	PA29	Kane Experimental Forest	6/1/2010	9/28/2010
NTN	PA29	Kane Experimental Forest	3/1/2011	
NTN	PA42	Leading Ridge	4/25/1979	
NTN	PA42	Leading Ridge	3/2/2010	
NTN	PA47	Millersville	11/21/2002	
NTN	PA47	Millersville	11/26/2002	
NTN	PA72	Milford	12/27/1983	
NTN	PA72	Milford	9/14/2000	
NTN	PR20	El Verde	2/12/1985	
NTN	SC05	Cape Romain National Wildlife Refuge	11/21/2000	
NTN	SC05	Cape Romain National Wildlife Refuge	3/2/2004	
NTN	SC05	Cape Romain National Wildlife Refuge	10/30/2007	
NTN	SC06	Santee National Wildlife Refuge	7/19/1984	
NTN	SC07	ACE Basin National Estuarine Research Reserve	12/31/2001	12/25/2007
NTN	SC11	North Inlet-Winyah Bay National Estuarine Research Reserve	1/8/2002	1/8/2009
NTN	SC99	Fort Johnson	3/19/2002	3/20/2007
NTN	SD04	Wind Cave National Park-Elk Mountain	11/5/2002	
NTN	SD08	Cottonwood	10/11/1983	
NTN	SD99	Huron Well Field	11/29/1983	
NTN	TN00	Walker Branch Watershed	3/11/1980	
NTN	TN00	Walker Branch Watershed	9/23/1992	
NTN	TN04	Speedwell	1/26/1999	
NTN	TN11	Great Smoky Mountains National Park-Elkmont	8/12/1980	
NTN	TN11	Great Smoky Mountains National Park-Elkmont	1/30/2002	
NTN	TN14	Hatchie National Wildlife Refuge	10/2/1984	
NTN	TX02	Muleshoe National Wildlife Refuge	6/18/1985	
NTN	TX03	Beeville	2/7/1984	
NTN	TX04	Big Bend National Park - K-Bar	4/10/1980	
NTN	TX10	Attwater Prairie Chicken National Wildlife Refuge	7/3/1984	
NTN	TX16	Sonora	6/26/1984	
NTN	TX21	Longview	6/29/1982	
NTN	TX21	Longview	3/12/1996	
NTN	TX22	Guadalupe Mountains National Park Frijole	6/5/1984	

		Ranger Station		
NTN	TX39	Texas A&M University-Corpus Christi	1/2/2002	12/26/2006
NTN	TX43	Cañónceta	7/24/2007	
NTN	TX43	Cañónceta	10/30/2007	
NTN	TX56	L.B.J. National Grasslands	9/20/1983	
NTN	UT01	Logan	12/6/1983	
NTN	UT08	Murphy Ridge	3/25/1986	
NTN	UT09	Canyonlands National Park-Island in the Sky	11/11/1997	
NTN	UT98	Green River	4/25/1985	
NTN	UT99	Bryce Canyon National Park-Repeater Hill	1/29/1985	
NTN	VA00	Charlottesville	10/2/1984	
NTN	VA10	Mason Neck	8/12/2003	7/14/2009
NTN	VA13	Horton's Station	7/25/1978	
NTN	VA24	Prince Edward	1/26/1999	
NTN	VA24	Prince Edward	3/1/2011	
NTN	VA27	James Madison University Farm	7/9/2002	6/30/2009
NTN	VA28	Shenandoah National Park-Big Meadows	5/12/1981	
NTN	VA28	Shenandoah National Park-Big Meadows	10/22/2002	
NTN	VA98	Harcum	8/31/2004	
NTN	VA98	Harcum	12/17/2004	
NTN	VA99	Natural Bridge Station	7/2/2002	
NTN	VI01	Virgin Islands National Park-Lind Point	4/14/1998	
NTN	VT01	Bennington	4/28/1981	
NTN	VT99	Underhill	6/12/1984	
NTN	VT99	Underhill	1/27/1993	
NTN	VT99	Underhill	7/27/2004	
NTN	VT99	Underhill	1/1/2008	
NTN	WA14	Olympic National Park-Hoh Ranger Station	5/20/1980	
NTN	WA19	North Cascades National Park-Marblemount Ranger Station	2/7/1984	
NTN	WA21	La Grande	4/24/1984	
NTN	WA24	Palouse Conservation Farm	8/20/1985	
NTN	WA98	Columbia River Gorge	5/7/2002	
NTN	WA99	Mount Rainier National Park-Tahoma Woods	10/26/1999	
NTN	WI09	Popple River	12/30/1986	
NTN	WI09	Popple River	3/6/1996	
NTN	WI10	Potawatomi	6/7/2005	
NTN	WI25	Suring	1/23/1985	
NTN	WI28	Lake Dubay	6/29/1982	
NTN	WI32	Middle Village	1/22/2002	3/28/2006
NTN	WI32	Middle Village	1/22/2002	3/30/2010
NTN	WI35	Perkinstown	1/26/1999	
NTN	WI36	Trout Lake	1/22/1980	
NTN	WI36	Trout Lake	3/5/1996	
NTN	WI37	Spooner	6/3/1980	
NTN	WI96	Wildcat Mountain YES	2/6/2007	
NTN	WI97	Lac Courte Oreilles Reservation	11/27/2001	3/22/2005

NTN	WI98	Wildcat Mountain	8/1/1989	
NTN	WI99	Lake Geneva	6/5/1984	
NTN	WI99	Lake Geneva	1/7/1997	
NTN	WV04	Babcock State Park	9/6/1983	
NTN	WV05	Cedar Creek State Park	1/26/1999	
NTN	WV18	Parsons	7/5/1978	
NTN	WY00	Snowy Range	4/22/1986	
NTN	WY02	Sinks Canyon	8/21/1984	
NTN	WY06	Pinedale	1/26/1982	
NTN	WY08	Yellowstone National Park-Tower Falls	6/5/1980	
NTN	WY08	Yellowstone National Park-Tower Falls	10/21/2004	
NTN	WY95	Brooklyn Lake	9/22/1992	
NTN	WY97	South Pass City	4/30/1985	
NTN	WY98	Gypsum Creek	12/26/1984	
NTN	WY99	Newcastle	8/11/1981	
SEARCH	CTR	Centreville	1/4/2005	1/1/2013
SEARCH	OAK	Oak Grove	1/4/2005	1/4/2011
SEARCH	OLF	Outlying Landing Field #8	1/4/2005	1/1/2013
SEARCH	YRK	Yorkville	1/4/2005	1/1/2013